

MORPHOLOGY AND CHEMISTRY
OF EARLY PRECAMBRIAN METABASALT FLOWS, UTIK LAKE, MANITOBA.

A Thesis
Presented to the
Faculty of Graduate Studies
of
The University of Manitoba

In Partial Fulfillment
of the Requirements
for the degree
Master of Science

by
ROY HARGREAVES

August, 1978



MORPHOLOGY AND CHEMISTRY
OF EARLY PRECAMBRIAN METABASALT FLOWS, UTIK LAKE, MANITOBA

BY

ROY HARGREAVES

A dissertation submitted to the Faculty of Graduate Studies of
the University of Manitoba in partial fulfillment of the requirements
of the degree of

MASTER OF SCIENCE

© 1978

Permission has been granted to the LIBRARY OF THE UNIVERSITY OF MANITOBA to lend or sell copies of this dissertation, to the NATIONAL LIBRARY OF CANADA to microfilm this dissertation and to lend or sell copies of the film, and UNIVERSITY MICROFILMS to publish an abstract of this dissertation.

The author reserves other publication rights, and neither the dissertation nor extensive extracts from it may be printed or otherwise reproduced without the author's written permission.

(i)

ABSTRACT

A 400m thick, sequence of Early Precambrian, tholeiitic metabasalt flows consisting of interlayered massive and pillowed units was mapped in detail at Utik Lake, Manitoba.

Metamorphic grade is low to middle greenschist facies but most flows have preserved primary textures. A typical flow is composed of randomly oriented plagioclase laths (An_{55}) in a matrix of actinolite and minor iron-titanium oxide grains. The flows are aphyric, except for sparse pseudomorphosed pyroxene grains near the base of the thickest massive flow, and plagioclase microporphyritic textures in the lower parts of many massive flows. The central parts of other massive flows locally contain plagioclase laths with belt-buckle and swallow-tail morphologies suggestive of rapid cooling from a crystal-poor residual liquid in the flow. No chemical variations were observed across flows or between flows.

Flows consisting entirely of pillows have smooth to undulating upper surfaces and range in thickness from 1m to 100m. The thicker pillowed units may represent several pillowed flows, but flow contacts are difficult to define. Criteria which help define flow contacts include the presence of lateral zones of intrapillow cavities, conformable alteration zones, and thin (2cm) zones of hyaloclastite adjacent to pillow selvages.

Both discrete and interconnected two-dimensional pillow shapes are present but most pillows are probably interconnected in three dimensions. The pillows probably originated by a subaqueous budding process analogous to digitating subaerial pahoehoe toes.

Most massive flows have smooth upper surfaces and range in

(ii)

thickness from 3m to 35m. Individual flows comprise three zones: (1) a basal chilled zone, (2) a central massive zone, and (3) an upper chilled zone. Both upper and lower chilled surfaces vary in thickness and are independent of flow thickness. Basal chilled zones locally contain incipient pillows.

Some massive flows have strongly altered flow-top breccias. The alteration involved calcium addition, and is characterised by the presence of diopside, minor epidote and clinozoisite in interfragmental areas and replacing original material. This alteration, and other alteration present as fracture fillings and clots in some pillowed flows, may represent reaction with ocean water.

Most massive and pillowed flows extend across the entire area, a distance of 500m. Other flows are less extensive and terminate within the map area. In one observed flow termination, a massive flow abruptly changed into an interconnected pillowed flow unit. In some massive flows with brecciated tops, the breccia is absent near the inferred termination of the flow.

CONTENTS

	Page
Introduction	1
General statement	1
Processes of subaqueous basaltic volcanism	2
Location and access	5
Previous work	5
Method of study	5
Physiography	8
Acknowledgements	8
 Geologic setting	 10
 General petrography	 13
 Flow types	 13
Simple massive flows	13
Complex massive flows	21
Alteration	27
Petrography of massive flows	29
Pillowed flows	40
Introduction	40
Petrography of pillows	41
Internal and external structures	42
Pillow selvages	42
Interpillow voids	45
Hyaloclastite tuff	45
Concentric zoning	47
Intrapillow cavities	47
Relationship between pillows	50
Discrete pillows	50
Interconnected pillows	51
Pillow alteration	55
Origin of pillows	55
 Volcanic stratigraphy	 58
Introduction	58
Criteria for flow recognition	58
Lateral extent of flows	61
 Chemistry	 66
Introduction	66
Primary variations	66
 Alteration	 71
 Conclusions	 76
 References	 79

LIST OF FIGURES

	Page
1 Plan view and sections through a submarine pahoehoe flow	4
2 Map of study area and regional geology	6
3 Map of local geology of Utik Lake and Mistuhe Island	7
4 Composite section through various types of flows in formation 1	15
5 Outcrop diagram showing simple massive flow 20 grading laterally into interconnected pillows	17
6 Graph of maximum groundmass plagioclase size plotted against flow height	18
7 Photograph of subvertical cooling cracks at the top of simple massive flow 3	19
8 Photograph of a pillow that fills an open fracture at the top of simple massive flow 3	20
9 Outcrop diagram of altered pillowed flow 10 overlain by complex flow 11 with basal incipient pillows	22
10 Outcrop diagram of the flow-top breccia of complex flow 7 which thins and terminates	23
11 Photograph of a massive protrusion in the flow-top breccia of complex flow 9	25
12 Photograph of the flow-top breccia matrix of complex flow 8	26
13 Photograph of massive basalt blocks in the flow-top breccia of complex flow 9	28
14 Composite section depicting the petrographic features in a typical massive aphyric flow	32
15 Photomicrographs of a microporphyritic texture	35
16 Photomicrograph of a microlitic plagioclase lath with belt-buckle morphology	36
17 Photomicrograph of a microlitic plagioclase lath with swallow-tail morphology	37
18 Photomicrograph of a possible Schiller structure	39
19 Photomicrographs of variolites in pillows	43
20 Outcrop diagram of two pillows showing various internal structures	44
21 Photograph of an interpillow void filled with quartz	46
22 Photographs of pillows with intrapillow cavities	48
23 Outcrop sketches of irregular, interconnected pillows	52
24 Outcrop sketches of larger, irregular, interconnected pillows that may represent submarine lava tubes	53
25 Outcrop sketches of interconnected pillows showing the nature of their connections	54
26 Photograph of altered pillows from flow 4	56
27 Outcrop diagram of a pillowed flow underlain and overlain by massive flows	62
28 Plot of AFM ternary diagrams of complex flows 5 and 11 and simple flow 19	69
29 List of chemical changes during alteration of flow-top breccia	73

LIST OF PLATES

	location
1 The stratigraphy of north-central Mistuhe Island, Utik Lake, Manitoba	(in pocket)
2 Outcrop diagram of aphyric flows 2, 3 and 4	(in pocket)
3 Outcrop diagram of pillowed flow 6 which is overlain and underlain by complex flows 5 and 7	(in pocket)
4 Outcrop diagram showing pillowed flow 10#underlain and overlain by complex flows 9 and 11	(in pocket)
5 Flow thickness versus the chemical variation in flows 5, 11 and 19	(in pocket)

LIST OF TABLES

	Page
1 Types of flows in formation 1	14
2 Modal analyses of selected massive aphyric flow samples from flows 5, 11 and 19	30
3 Petrographic and morphologic features used to distinguish individual flows	59
4 Chemical analyses and Barth-Niggli normative values of samples from massive flows 5, 11 and 19	67, 68
5 Recalculated values of the altered samples	72

INTRODUCTION

General Statement

The Superior Province of the Canadian Shield consists partly of sinuous, east-trending metavolcanic-metasedimentary sequences of Early Precambrian age. Volcanic, volcanoclastic and sedimentary material are present in varying amounts and vary in relative proportions from sequence to sequence. Most sequences are isoclinally folded and have faulted and/or intrusive contacts with the surrounding granitic rocks that make up most of the Superior Province. The sequences appear to be only remnants of large deformed volcanoes, but they are amenable to study because the upright isoclinal folds and glaciated surfaces provide good cross-sections, and because primary structures and textures are well preserved despite the folding and greenschist facies metamorphism. In order to understand better the history of these supracrustal rocks, the stratigraphy, morphology and depositional environments of individual units and of the sequences must be documented more fully. Recent major contributions in this field have been made by Barager (1968), Boutcher et al, (1966), Goodwin (1962; 1966; 1968a; 1968b) and Wilson et al, (1974) among others.

In this thesis, the author will document the vertical and lateral morphological variations in a 400m thick sequence of massive and pillowed basaltic flows. Chemical and petrographic variations through selected flows have been determined with special emphasis being placed on pre-metamorphism alteration. Recent investigations of Early Precambrian basaltic flows have also been made by Pearce (1974), Pearce and Birkett (1974), Gelinis and Brooks (1974), Pyke et al, (1973), Côté and Dimroth (1976), and Dimroth et al, (1978).

Processes of Subaqueous Basaltic Volcanism.

Subaqueous volcanism dominates modern volcanic regimes, but the processes are poorly known because of the inherent difficulty of examination. Much of our data about subaqueous volcanism comes from uplifted subaqueous sequences. In this regard, the Early Precambrian metavolcanic sequences are excellent sources of information because the isoclinal folding has produced cross-sections through thick subaqueous sequences.

Many Early Precambrian and younger basaltic sequences consist of intimately interlayered massive and pillowed units but the precise relationship and genesis of these units is not well documented. In some areas the pillowed and massive units represent discrete flows but in other areas they are combined in various proportions to form complex flows (Dimroth et al, 1978; Côté and Dimroth, 1976; Cook, James and Mawdsley, 1931; and Wilson, 1942).

The origin of pillows is controversial, particularly in the Early Precambrian (Jones, 1968; Johnston, 1969) because until recently, (Moore et al, 1973; Moore, 1975), pillows had not been observed during formation. Many ideas on pillow development have been postulated since the inception of the term pillow by Cole and Gregory (1890) and many hypotheses were discussed in Lewis' (1914) classic paper. Some of these are hypothetical mechanisms whereas others are based on observed processes. Throughout the years, two schools of thought have developed and differ in whether pillows are discrete individuals (Johnston, 1969) or are connected to other pillows (Jones, 1968; Moore et al, 1973; Moore, 1975; Vuagnat, 1975). The controversy has arisen because many Early Precambrian exposures are two dimensional and show mainly discrete

pillows whereas many younger flows have three-dimensional exposures and are mainly interconnected. Both types of pillows may exist, but the apparent discrete nature of many Early Precambrian pillows may be an artifact of the two-dimensional exposure, and incomplete examination.

Observations of advancing submarine pahoehoe flows at Hawaii (Moore, 1975) and of well exposed ancient pillowed flows (Jones, 1968) indicate that most if not all pillows are produced by a submarine mechanism similar to the digital advance of subaerial pahoehoe toes. By this mechanism, lava moves through interconnected lava tubes to the flow front where the tube ruptures and a small amount of lava is extruded to form a pillow. Each pillow is connected to other pillows except for a few pillows that break off to form discrete entities. The pillows generally trend downslope, but form a complex entrail-like pattern (Fig. 1). Because of this pattern, a two-dimensional section through a pillowed sequence will produce pillows that appear to be either discrete or interconnected, depending on the eroded view of the pillow. This is particularly important when determining the origin of pillows in glaciated sequences of the Canadian Shield where only two-dimensional pillow shapes are generally visible. Pillowed units eroded perpendicular to flow direction would exhibit many apparently discrete pillows and only a few pillows would show connections to other pillows. An eroded section parallel to the movement direction would also show many apparently discrete pillows because of the entrail-like pattern but there would be more connected pillows than in a perpendicular section (Fig. 1). Thus the presence of some interconnected pillows within a pillowed flow infers that most pillows in that flow are connected, and were formed by the digital advance of submarine pahoehoe.

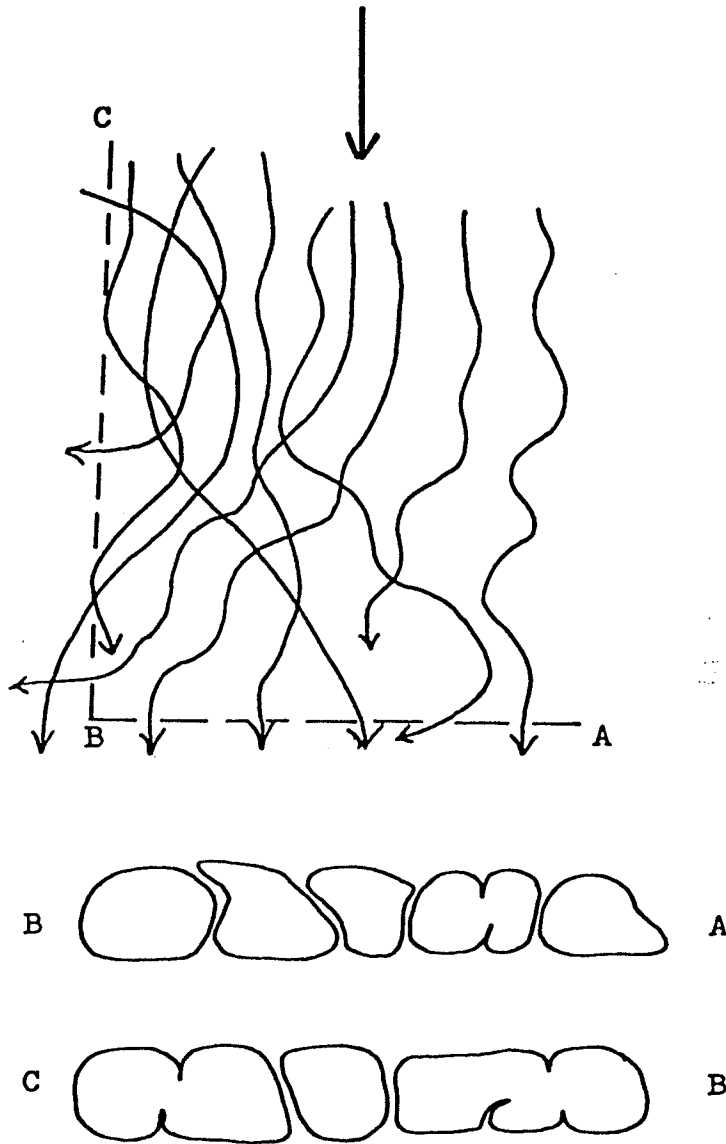


Figure 1. A plan view (top) and sections BA and CB through an entrail-like submarine pahoehoe flow. The curved lines in the plan view represent the paths taken by individual pillows and the arrow-heads indicate their movement direction. Section BA is perpendicular to the general movement direction (heavy arrow) and shows that the majority of pillows are apparently discrete entities whereas section CB parallel to movement direction shows the pillows to be mostly interconnected. Because of the curving of individual pillows, the section parallel to the general flow direction still shows pillows cross-sections rather than longitudinal sections.

The fact that differently oriented sections through a pillowed flow yield apparently different types of pillows partly explains why geologists cannot agree on whether pillows are discrete (Johnston, 1969) or interconnected (Jones, 1968).

LOCATION AND ACCESS

Utik Lake is 130km east of Thompson, Manitoba (Fig. 2). The area mapped is on Mistuhe Island, a recently burned island near the southern edge of the lake (Fig. 3). Access was by float-equipped aircraft from Thompson.

PREVIOUS WORK

Little geological work was done at Utik Lake prior to 1951 when Milligan (1952); Allen (1953); and Milligan and Take (1954) mapped various portions of the Utik Lake-Bear Lake area. Quinn (1955) also mapped the area as part of a regional geological study of the Knee Lake area. The most recent work was done by Weber (1974a, 1974b).

METHOD OF STUDY

An area 2km^2 was mapped at various scales during the summers of 1974 (Hargreaves, 1974), 1975 (Hargreaves, 1975a, 1975b), and the fall of 1976 (Hargreaves, 1976). Three weeks were spent mapping the sequence on specially flown 1:4000 air photographs. Another seven weeks were required to map the aphyric sequence at 1:1200 scale. Three stratigraphic sections were measured, and 1:60 detailed outcrop maps were prepared where warranted.

Double fist-sized samples were collected at 2m vertical intervals through each massive flow in each section. Pillowed flows were sampled by collecting material from the centers of four similar-sized pillows

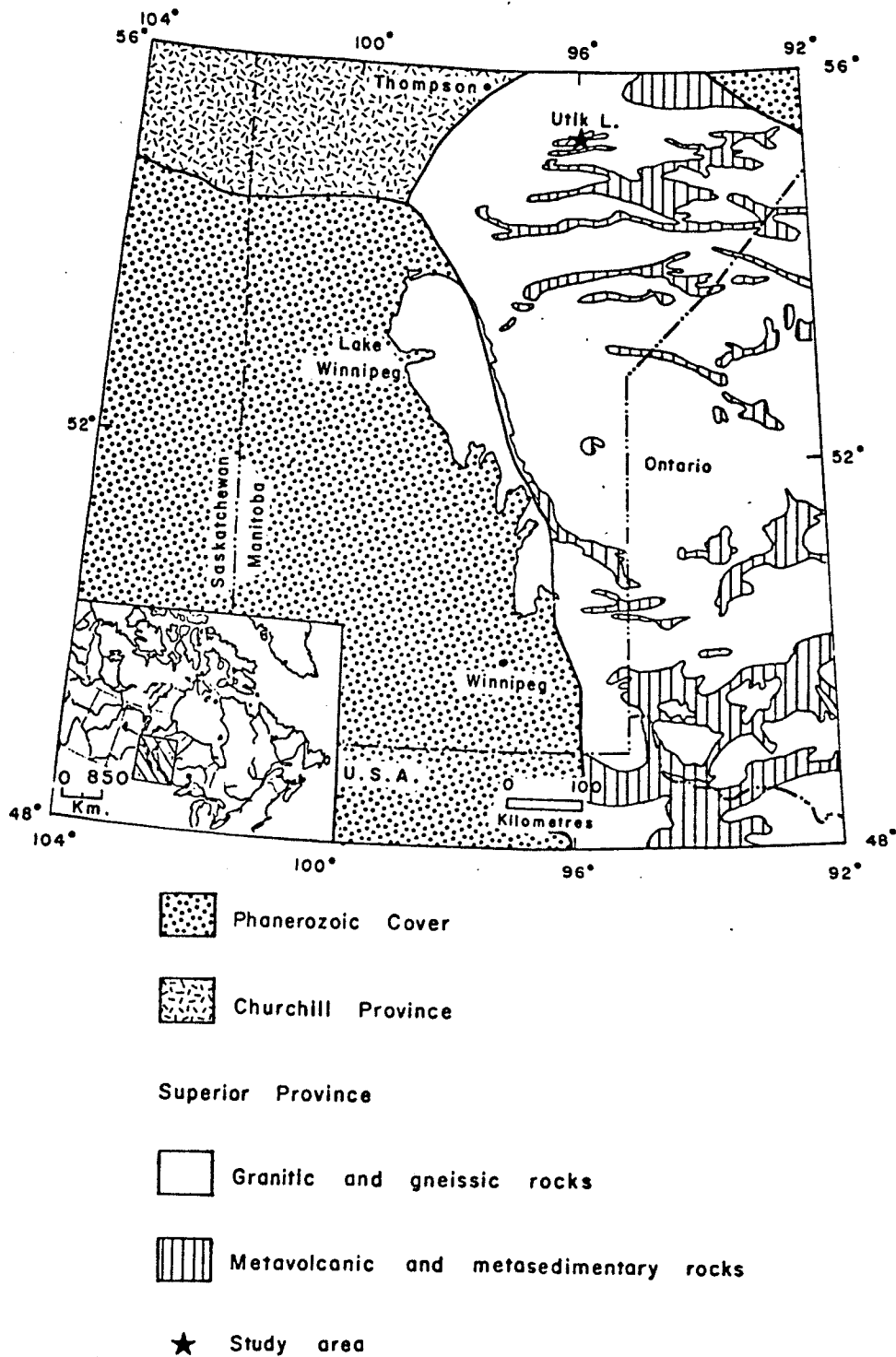
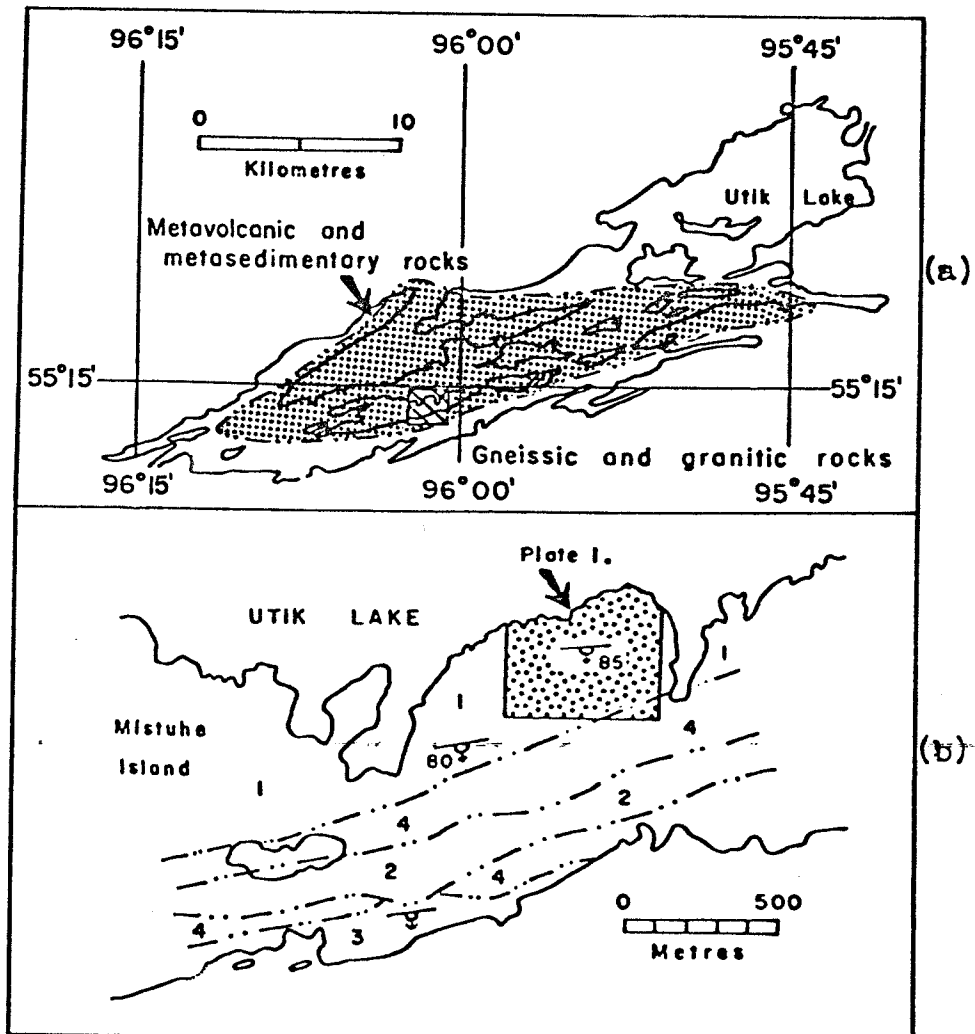


Figure 2. Map showing study area and regional geology.



- 4 Gabbro
- 3 Bedded intermediate tuff, lapillstone and pillowed porphyritic basalt
- 2 Massive and pillowed porphyritic basalt with iron formation
- 1 Interlayered massive and pillowed aphyric basalt with flow-top breccia
- Geological contact
- 85° Strike and dip of inclined pillowed lava flows, top known

Figure 3. The local geology of (a) Utik Lake and (b) Mistuhe Island outlining the area of intensive study.

(1m to 1.5m in length) in order to establish consistency. The selvages, amygdules, variolites and interpillow and intrapillow cavity material were also sampled where possible.

Over 400 thin sections were examined and 24 samples were chemically analysed. The analyses were carried out in the Department of Earth Science Laboratories, University of Manitoba under the supervision of K. Ramlal utilising X-Ray Fluorescence and wet chemical techniques.

PHYSIOGRAPHY

An extensive cover of glacial drift, sand, and clay has left much of Utik Lake with very low relief, and only along the southern edge of the lake does relief exceed 25m. Local wave action has cleaned most shoreline exposure, but inland exposures are rare and where present are heavily lichen-covered.

A forest fire in 1973 on Mistuhe Island destroyed the vegetation, and removed the lichen cover from inland outcrops which are more abundant than in most other parts of the Utik Lake area. In the intensively studied area (Plate 1) exposure is about 20 percent and is exceptionally clean. Swamps and muskegs are dry, permitting easy access to the center of the island.

ACKNOWLEDGEMENTS

The author would like to thank the Manitoba Mineral Resources Division, especially W. Weber, for partial logistical support during the 1974 and 1975 field seasons. The remainder of the field support was provided by N.R.C. grant A 8996 to L.D. Ayres. The author would like to thank members of the Department of Earth Science Laboratories for doing the X-Ray Fluorescence and the wet chemical analyses.

Capable assistance was rendered in the field by T. McDonald, C. Cutforth and U. Hamann in 1974; and by the late W. Foidart in 1975. The author would also like to thank S.R. Smith, who accompanied him in the field during the fall of 1976.

Special thanks to L.D. Ayres, D. Car, T. Pearce and W. Weber for critical discussions about various aspects of the problem; Ayres and Weber visited the author in the field.

The manuscript was critically reviewed by L.D. Ayres, W.C. Brisbin and E. Chow.

GEOLOGIC SETTING

The Utik Lake metavolcanic-metasedimentary sequence is thought to be a continuation of the Hayes River Group (Milligan and Take, 1954), first documented by Wright (1925) at Island Lake. The portion exposed at Utik Lake is wedge-shaped and has a maximum width of 5km (Fig. 3). It is an east-trending, vertically dipping, south-facing homocline. Four mafic volcanic cycles are exposed, each separated by a period of quiescence, during which volcanically derived conglomerate, greywacke and mudstone were deposited. Numerous synvolcanic gabbro and quartz-feldspar porphyry plutons intruded the volcanic sequence, and are most likely related to volcanism higher in the sequence. Large massive to foliated granodiorite plutons with cupolas of alaskite intruded the sequence and now form its margins. These granitic plutons separate the metavolcanic-metasedimentary sequence from an extensive gneissic terrain.

The metavolcanic rocks are generally poorly exposed, but exceptionally good exposure occurs on Mistuhe Island where the uppermost volcanic cycle is exposed. Formations exposed on Mistuhe Island include:

Formation	Description	Thickness (metres)
4	Differentiated metagabbro sill	300
3	Bedded intermediate tuff, lapillistone and pillowed porphyritic basalt flows	90
2	Massive and pillowed porphyritic basalt flows with interflow iron formation	110
1	Interlayered massive and pillowed aphyric basalt flows	400

On Mistuhe Island the formations trend 085°, are vertically

dipping and become successively younger southward (Fig. 3b). Although the sequence is part of an isoclinal fold, flow-top breccias and pillows are only slightly deformed. Metamorphic grade varies from hornblende-hornfels facies south of the island to albite-epidote-hornfels facies along the northern shore. Foliation is absent, with plagioclase laths and actinolite growths having felted and random habits respectively.

Formation 1 consists of intimately interlayered massive and pillowed aphyric basalt flows. Massive flows range in thickness from 3m to 35m, and pillowed flows from 1m to 100m, although some of the thicker pillowed sequences may represent several flows.

In formation 2, massive and pillowed porphyritic flows range in thickness from 2m to 27m, and contain tabular plagioclase phenocrysts or xenocrysts up to 4cm long. Further west, the phenocrysts are up to 12cm long. The phenocrysts are concentrated in a 1m to 2m thick zone near the top of the flows where they form up to 15 percent of the flow. They decrease in abundance downward, and the average phenocryst content is about 3 percent. Most phenocrysts are recrystallised and partly altered to sericite, but one relatively fresh crystal was Labradorite (An_{60}). Locally, porphyritic massive flows are separated by penecontemporaneously deformed iron formation units. Basalt immediately below the iron formation is commonly altered to a fine-grained, white to rusty weathering material containing abundant garnet and anthophyllite (Weber, 1974a). Similar white weathering material occupies joints and fractures in the upper part of the flow.

Pillowed porphyritic flows increase in abundance southward relative to massive flows, and are interlayered with bedded intermediate tuff, lapillistone, and iron formation of formation 3.

A differentiated metagabbro sill (formation 4) and smaller related sills were emplaced along the contact between formations 1 and 2. Four distinct zones are present in the main sill: (1), a basal clotted gabbro, (2) coarse-grained gabbro, (3) medium-grained gabbro, and (4) a capping pegmatitic gabbro. Gravity settling appears to have been the main agent of differentiation, and the pegmatitic gabbro was the last part of the sill to crystallize.

A minor swarm of feldspar porphyry dikes striking 170° occurs within the aphyric flow sequence along the north shore of the island. These grey-coloured dikes rarely exceed 1m in width, and can be traced across two or three flows. One such dike near the top of the aphyric sequence contained xenoliths of massive medium-grained granite.

Only formation 1 is well exposed and commonly shows complete sections through one or more flows on the larger outcrops. Exposures of this type are essential to flow morphology studies, and the remainder of this thesis will be devoted to these aphyric flows.

GENERAL PETROGRAPHY

The aphyric basalt in formation 1 weathers deep olive green and is black on fresh surfaces. It is fine to medium-grained (up to 2mm) and consists of 30 to 40 percent plagioclase, 55 to 65 percent actinolite, 5 percent iron-titanium oxide, and minor sphene, biotite and epidote. Plagioclase is the only mineral that retains its primary shape of felted laths and microlites, but primary textures are not preserved in all flows. The actinolite forms blades and prisms that probably replaced original pyroxene and glass.

FLOW TYPES

Thirty-six flows have been recognized in formation 1 (Plate 1, in pocket). Of these, 13 are pillowed and comprise 38 percent of the sequence; the remaining 23 flows are massive (Table 1). Massive flows are of two basic types: simple flows that have lower and upper chilled zones but lack other major structural features, and complex flows which have an upper flow-top breccia. Both types of massive flows can have incipient pillows in their lower chilled zones (Fig. 4). The three flow types are interlayered as either single flows or sequences of several flows (Plate 1), and are treated collectively from this point onwards.

Flows range in thickness from 3m to 35m for massive flows and from 1m to 100m for pillowed flows, although some of the thicker pillowed units may represent several flows.

Simple Massive Flows

These flows have a very fine-grained (0.05mm) basal chilled zone up to 30cm thick. Incipient basal pillows are present locally in the chilled zone and appear as attached pillow-like forms or deeply

Table 1. Types of Flows in Formation 1

(1) This includes the lowermost 26 flows on Plate 1, for which thickness data are most reliable.

Flow Type	Total number	Total thickness	Percentage of Sequence ¹	
			by number	by thickness
Pillowed flows	13	135m	38%	46%
Massive flows (total)	23	265m	62%	54%
Simple massive flows (total)	13	112m	31%	23%
with chilled base and top	13		27%	20%
with chilled base and top and basal incipient pillows	2		4%	3%
Complex massive flows (total)	10	153m	31%	31%
with flow-top breccia	10		23%	16%
with flow-top breccia and basal incipient pillows	2		8%	15%

CONTACTS & INTERNAL CHARACTERISTICS

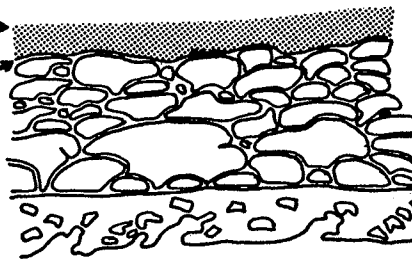
undulating surface



FLOW TYPE

Simple Massive Flow

chill zone
flat base



Pillowed Flow

central massive zone

Complex Massive Flow

basal pillowed zone

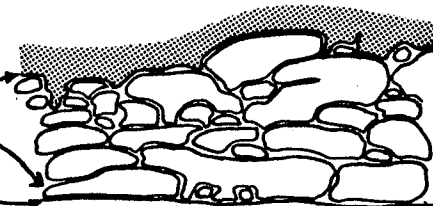


Complex Massive Flow

undulating base

flat-based pillows

flat surface



Pillowed Flow

Massive Flow

Figure 4. Composite section showing the various types of flows in formation 1, their internal characteristics, and the nature of their contacts.

re-entrant selvages that resemble the sides and bases of pillows (flow 21 in Fig. 5). The incipient pillows form a one pillow thick, discontinuous layer less than 0.5m thick. They may represent rapid digital advance of the flow where the upper selvages of the basal pillows, and any higher pillows have been remelted by the hot interior of the flow.

Basal chilled zones weather lighter green than the bulk of the flow and grade rapidly upward into a coarser central zone where groundmass plagioclase is up to 2mm long (Fig. 6). The upper chilled zone weathers dark green, and is the same colour as the interior of the flow. It is not readily apparent in outcrop, but a very fine grain size (0.05mm) was noted in the matrix. Quartz-filled amygdules are rarely present.

In the upper surface of flow 3 (Plate 2, in pocket) cooling fractures 1mm to 1m wide (Fig. 7) and up to 2m deep were observed. These fractures have a spacing of 15cm and vary from perpendicular to slightly inclined to the flow surface; minor subsidiary fractures parallel to the flow surface are also present. A white weathering calcium-rich diopside-epidote-clinozoisite alteration lines the fractures. Some of the wider fractures (0.3m to 1m in width) contain pillows that are completely surrounded by selvage. The viscosity of these pillows must have been low because the pillows conform to the shape of the cracks (Fig. 8). These pillows are probably related to the overlying pillowed flow but could also represent a type of squeeze-up in the massive flow. The fact that some of the cooling fractures developed into wide cracks indicates that some flow movement occurred after the fractures first developed. Similar cracks were not

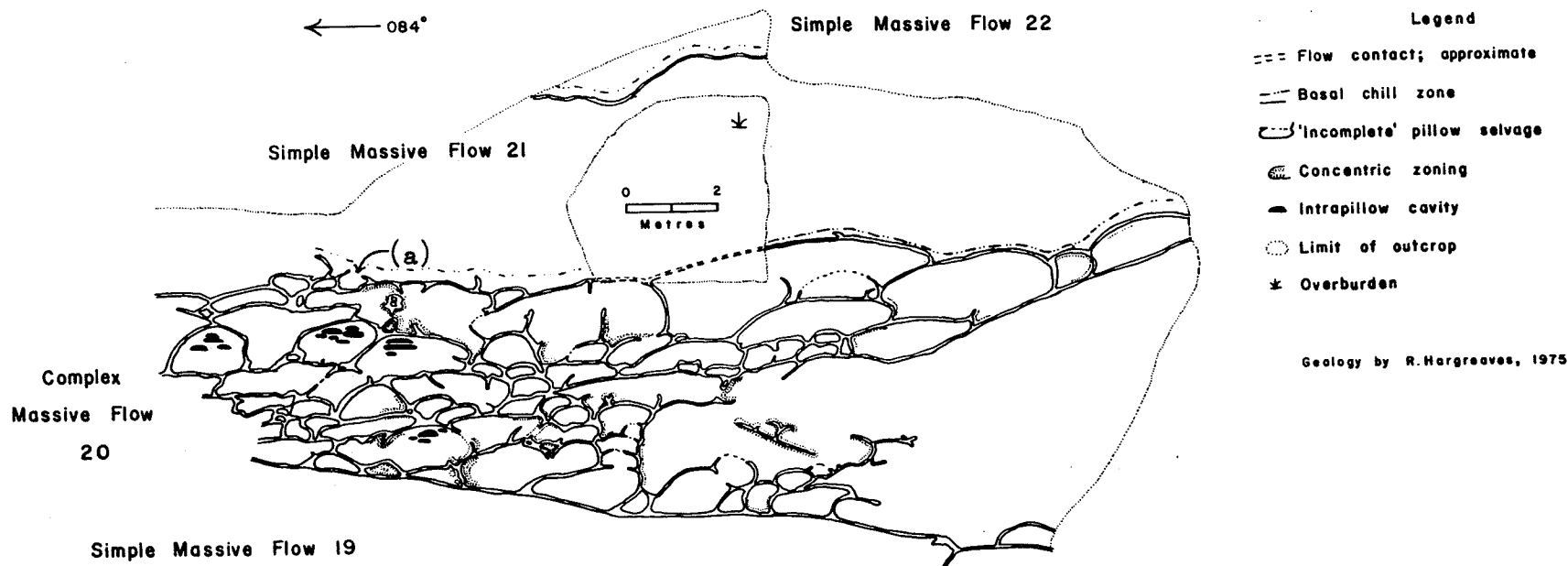


Figure 5. Outcrop diagram showing massive flow 20 underlain and overlain by simple massive flows. Flow 20 consists of a massive flow that grades laterally into interconnected pillows. Note the flat-based pillows at the bottom of the pillowed unit and the slight inclination of the pillows. The flow surface of flow 19 is flat whereas flow 21 has an undulating surface. Note the incipient pillow at the base of flow 21 (a).

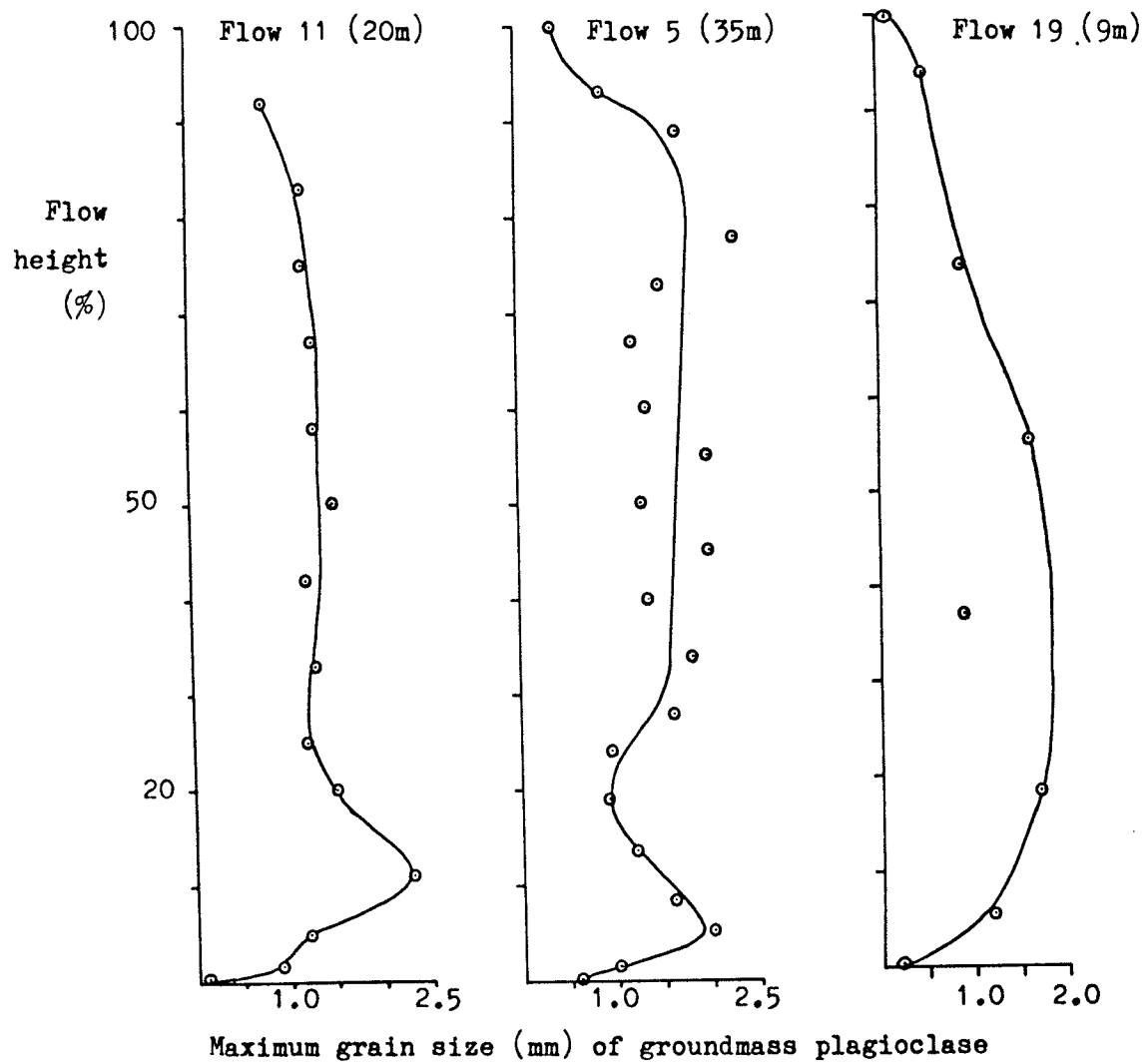
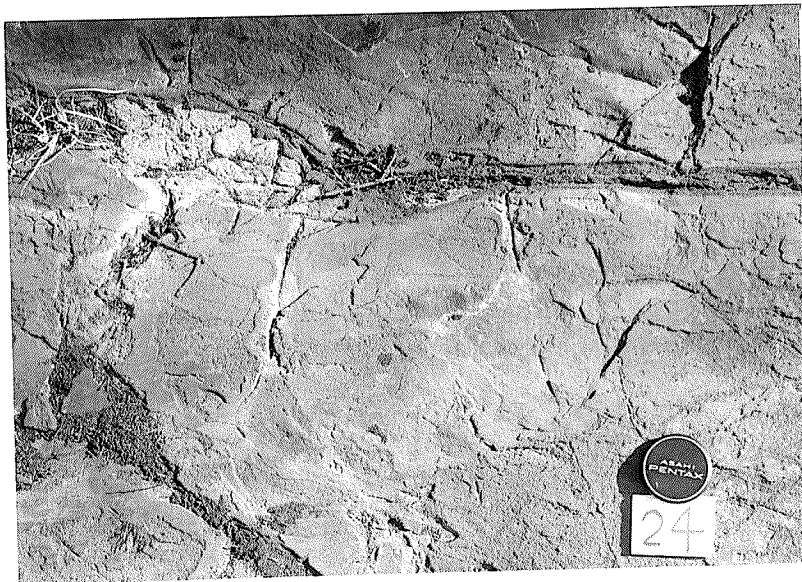


Figure 6. Graph of maximum groundmass plagioclase size plotted against flow height.



(a)



(b)

Figure 7. Subvertical cooling cracks (a) and open fractures (b) present along the flat top of simple massive flow 3. The cracks are rimmed by white weathering diopside-epidote-clinozoisite alteration. Lens cap measures 55mm.



Figure 8. Pillow that fills an open fracture at the top of simple massive flow 3. Note the white weathering alteration (light tone) at the side of the pillow and the intrapillow cavity near the top of the pillow. Lens cap (55mm) for scale.

observed in the other simple massive flows.

A 2cm thick hyaloclastite tuff unit occurs along the undulating surface of flow 21. Individual grains in the tuff are up to 1.5cm and consist of equal amounts of bladed actinolite (0.3mm in length) and inequigranular plagioclase (0.1mm). The tuff probably formed from quenching and granulation of the upper surface of the flow.

Complex Massive Flows

These flows consist of three major parts: (1) a basal chilled zone that contains local incipient pillows, (2) a coarser grained central massive zone and (3), a flow-top breccia (Fig. 4). Within individual flows, the flow-top breccia and the basal chilled zone pinch and swell and are locally absent. Incipient pillows are not present in all flows (Table 1). The thickness of both the breccia and the incipient pillow layers are independent of flow thickness.

The basal chilled zone is identical in thickness, grain size and development of incipient pillows to that in simple flows (Figs. 9, 10). In several flows, zones of alternating light and dark green laminae up to 12cm thick are locally present immediately above the flow base (Fig. 9). These zones can be traced laterally for only 0.2m and appear to grade laterally and vertically into normal chilled basalt. Individual laminae are 3mm thick, and represent grain size variations with the finer, dark green layers consisting of an inequigranular mosaic (0.07mm) of plagioclase and actinolite and the coarser light green layers consisting of poorly formed plagioclase laths (0.14mm in length) and actinolite prisms and blades (0.15mm to 0.20mm in size). This layering probably represents primary flow layering and its disappearance laterally could be due to metamorphism

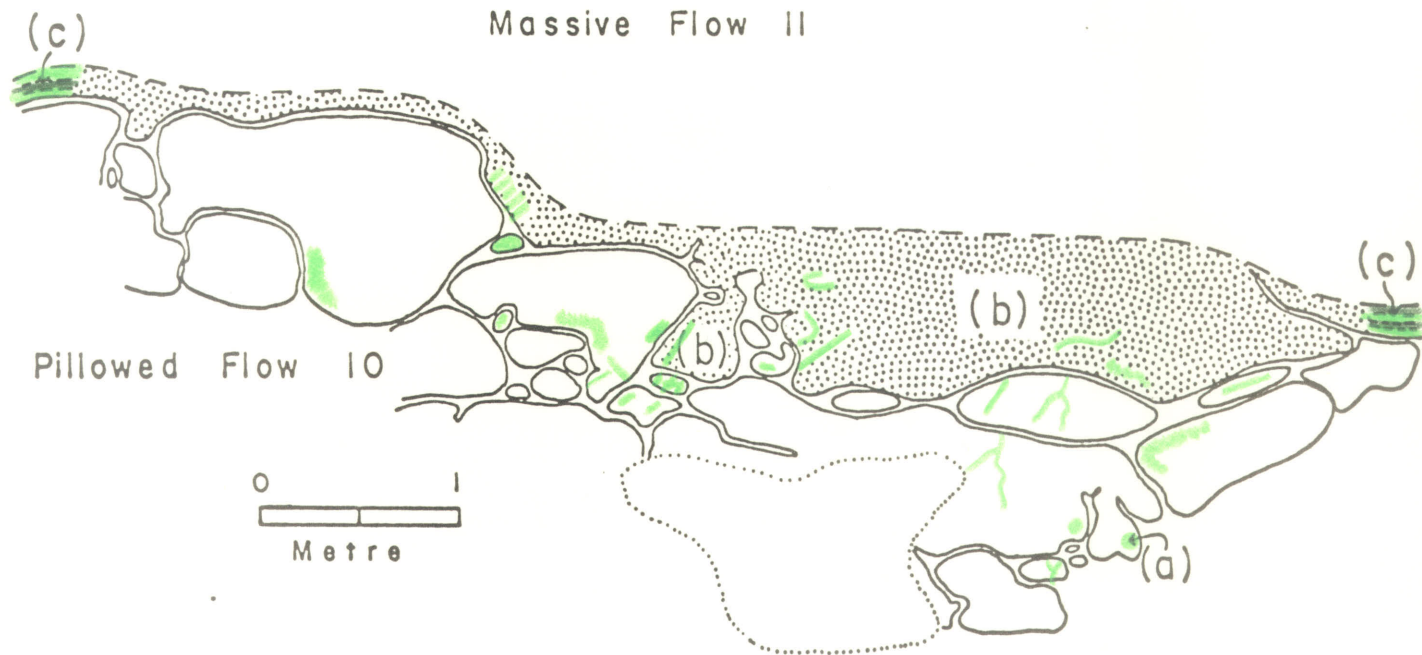


Figure 9. A pillowed flow that has an undulating upper surface and local alteration (a). It is overlain by a complex massive flow. Note the basal incipient pillows (b) and alternating light and dark green laminae (c) in the basal chilled zone (stipled).

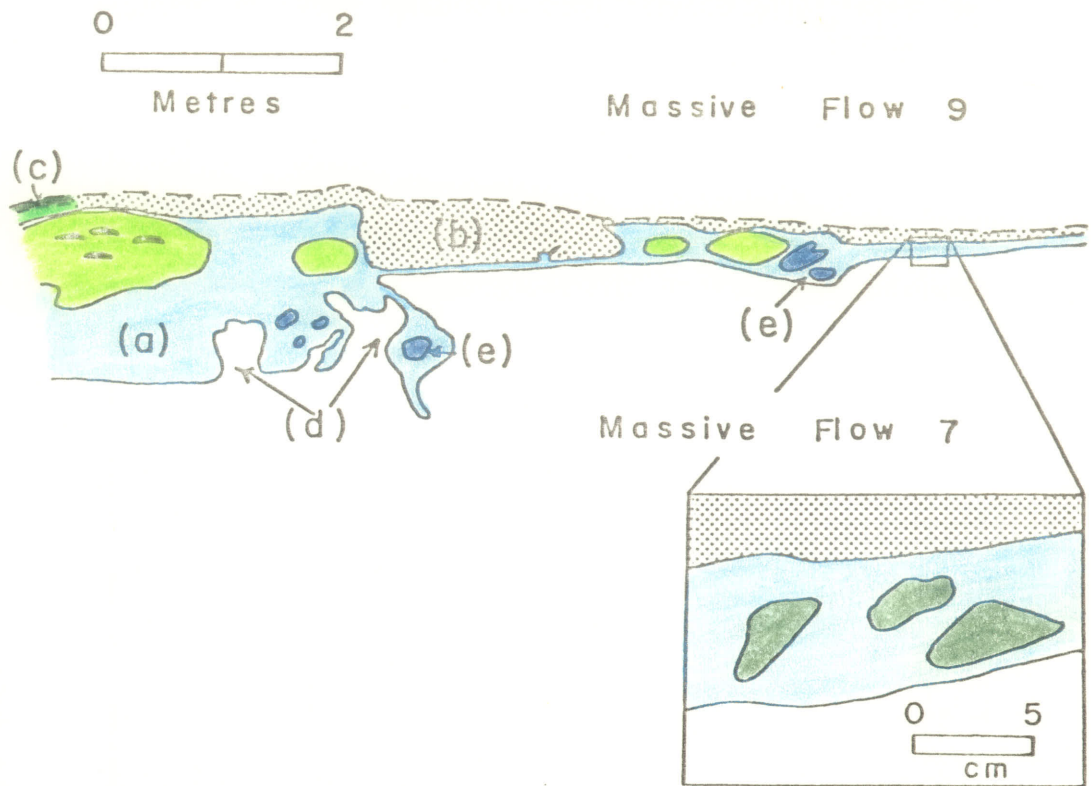


Figure 10. A complex massive flow with flow-top breccia (a) overlain by another complex massive flow that has basal incipient pillows (b) and alternating light and dark green laminae (c) in the basal chilled zone (stippled). Note the massive protrusions (d), white altered massive basalt fragments (e) and whole pillows (light green) within the breccia. Where the breccia is thin (inset) it is composed of apparently unaltered massive fragments (green) in a dark green granular matrix.

or to a combination of pre-metamorphism alteration and metamorphism. Above the chilled zone, grain size increases upward from less than 0.5mm to more than 2mm in the central massive zone (Fig. 6) and then decreases to 0.8mm below the breccia.

Flow-top breccia zones range in thickness from 0.3m to more than 3m. Locally, they pinch and swell, and in one flow the breccia unit thins from more than 1m to only 6cm in a lateral distance of 6m (Fig. 10).

The breccias have a general composition of 15 percent white weathering angular to rounded altered basalt blocks, 50 percent green-weathering, less altered basalt blocks and lapilli; and 35 percent light green alteration material as cement. The contact between the central massive zone and the breccia is irregular (Fig. 10, and Plate 3, in pocket). This irregularity largely reflects upward protrusions of massive basalt that extend into the lower half of the breccia unit from the top of the central massive zone (Fig. 11). In some flows elsewhere in the Superior Province, similar protrusions were found to have a consistent dip, and the inclination of the protrusion might be used as a guide to the direction of flow movement (Côté and Dimroth, 1976). Recent subaerial aa flows have similar protrusions that are inclined upwards in the direction of flow (Macdonald, 1967). In Mistuhe Island complex flows, the protrusions have vertical or non-uniform inclinations and are not useable for determination of flow direction.

The dark green lapilli and blocks have a maximum size of 15cm. These clinkery fragments predominate in the flow-top breccia and vary in shape from ovoid to rectangular (Fig. 12). Individual fragments are composed of bladed actinolite up to 1mm long and minor inequigranular



Figure 11. A white weathering massive protrusion into the base of the flow-top breccia (deep green) of complex massive flow 9; 55mm lens cap for scale.



Figure 12. The flow-top breccia matrix of complex massive flow 8. Note the lapilli and block-sized clinkery fragments (dark tone) and the surrounding alteration material (light tone). Lens cap (55mm) for scale.

plagioclase anhedral 0.3mm in size. Iron-titanium oxide grains are rare, but where observed are rimmed by anhedral sphene. The lapilli probably represent the glassy surface of the flow that became brecciated as the flow moved.

The white weathering fragments are strongly altered and range in size from 5cm to 30cm (Fig. 13); they are generally larger than the dark green fragments. Some fragments are bent and were probably deformed while still hot. The fragments have partial black selvages and have the general appearance of broken pillows similar to those found in pillow breccias. However, the breccia is an integral part of the flow and is not a typical pillow breccia. There are local concentrations of white fragments with these fragments forming 50 to 80 percent of the breccia. These fragment-rich areas probably represent brecciated massive protrusions. The less abundant, more scattered white fragments elsewhere in the breccia probably had a similar origin.

Whole pillows with complete selvages are present in the flow-top breccia of flow 7 (Fig. 10), but these are possibly related to a later pillowed flow that burrowed into the breccia or are a squeeze up phenomenon related to the late stages of the brecciated flow.

Alteration

The flow-top breccias are intensely altered. The alteration is concentrated in white weathering massive basalt blocks and the light green cement. The dark green fragments have very little alteration. If the white weathering blocks are massive protrusions that were intruded and brecciated while still hot, then ocean water percolating through the breccia may have caused intense alteration of the hot basalt. The



Figure 13. Angular to sub-rounded, white weathering, massive basalt blocks in the flow-top breccia of complex massive flow 9. White 13cm rule for scale.

dark green fragments probably represent the brecciated surface of the flow and would have been much cooler when in contact with ocean water. In modern subaqueous basaltic flows that are being altered by ocean water, the intensity of alteration is proportional to the temperature of the flow (Scott and Hajash, 1976).

In the white weathering massive basalt blocks, inequigranular diopside (up to 1mm in size) is present rather than actinolite and poikilitically encloses slightly corroded plagioclase laths (0.8mm) that do not appear to have been affected by the alteration. Anhedral epidote and clinozoisite are locally present in the diopside and euhedral sphene has overgrown iron-titanium oxide grains.

The cement that surrounds both the white basalt blocks and the dark green fragments consists of fine to medium-grained diopside (2mm) epidote (0.8mm), clinozoisite laths (0.3mm in length), and minor anhedral calcite (0.3mm). The calcite appears to fill voids and may be a later secondary mineral not related to the actual alteration.

The chemistry of the alteration will be discussed in a subsequent section.

Petrography of Massive Flows

Massive and pillowed flows are mineralogically similar and are composed of light to deep green actinolite, plagioclase, iron-titanium oxide grains and trace amounts of rutile, sphene and biotite (Table 2). Most plagioclase still retains its primary shape and composition but the other primary minerals have been recrystallized or replaced by metamorphic minerals.

In massive flows the actinolite content ranges from 62 to 71 percent and plagioclase content from 27 to 35 percent. Within most

Table 2. Modal analyses of selected massive aphyric flow samples submitted for chemical analysis.

Samples are arranged from the flow base (5-1) upwards to the flow top (5-10). Location of flows are on Plate 1 and are flow 19 (1-5), flow 11 (6-14), and flow 5 (15-24). Samples 5-1, 11-1, and 19-1 represent chilled bases and 19-5 represents the chilled surface of a simple flow. Samples 5-10 and 11-9 are flow-top breccia matrix samples whereas 11-8 is an altered massive basalt fragment.

	FLOW 5										FLOW 11								FLOW 19					
	5-1	5-2	5-3	5-4	5-5	5-6	5-7	5-8	5-9	5-10	11-1	11-2	11-3	11-4	11-5	11-6	11-7	11-8	11-9	19-1	19-2	19-3	19-4	19-5
Plagioclase	32.0	31.1	32.3	26.6	26.6	25.5	18.8	20.9	13.5	P.	36.2	33.3	35.0	35.3	34.0	33.7	33.4	P	P	30.0	36.9	37.5	39.9	30.8
Actinolite	66.4	65.5	65.1	67.6	70.1	71.9	77.5	76.3	80.3	P	63.2	64.7	62.6	62.3	62.1	64.0	62.7	P	P	64.3	60.2	59.7	58.1	66.7
Biotite	-	1.0	-	-	-	-	-	-	-	T	-	0.1	-	0.3	-	0.2	-	-	T	2.2	0.6	-	0.1	-
Fe-Ti oxide	1.0	2.2	2.2	5.6	3.3	2.6	3.0	2.2	5.3	P	-	0.1	2.1	2.0	2.8	2.0	2.9	P	P	2.9	1.6	2.4	1.8	0.1
Rutile	0.6	0.2	0.4	0.2	-	-	0.7	0.6	0.7	-	-	0.3	0.3	0.1	-	0.1	0.8	-	-	0.6	0.7	0.4	0.1	-
Sphene	-	-	-	-	-	-	-	-	-	P	-	-	-	-	-	-	0.2	P	P	-	-	-	-	-
Diopside	-	-	-	-	-	-	-	-	-	P	-	-	-	-	-	-	-	P	P	-	-	-	-	-
Epidote	-	-	-	-	-	-	-	-	-	P	-	-	-	-	0.1	-	-	P	P	-	-	-	-	-
Clinzoisite	-	-	-	-	-	-	-	-	-	P	-	-	-	-	-	-	-	P	P	-	-	-	-	-
Calcite	-	-	-	-	-	-	-	-	-	P	-	0.1	-	-	-	-	-	-	P	-	-	-	-	-
Quartz veins	-	-	-	-	-	-	-	-	-	-	-	-	-	-	-	-	-	T	-	-	-	-	-	0.1
Quartz vesicles	-	-	-	-	-	-	-	-	0.1	-	-	-	-	-	-	-	-	-	-	-	-	-	-	0.1
Plagioclase veins	-	-	-	-	-	-	-	-	0.1	-	-	-	-	-	-	-	-	-	-	-	-	-	-	2.2

REMARKS

Modal analyses conducted in a 5mm x 15mm area using 1500 points

Samples 5-10 and 11-9 are too inhomogenous to modally analyse

Sample 11-8 is too fine-grained to modally analyse

P = minerals present (>1%)

T = trace amounts (<1%)

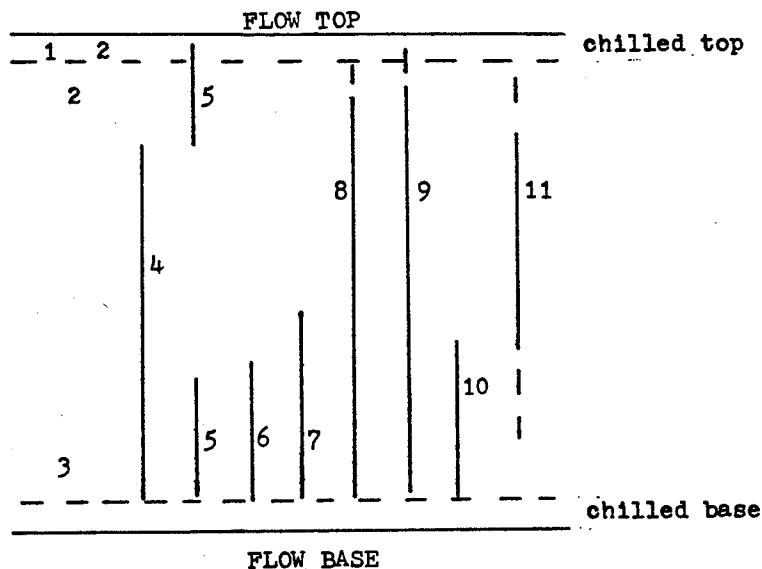
flows, the actinolite:plagioclase ratio is relatively constant throughout the flow but in the thickest flow (flow 5, 35m), actinolite and plagioclase contents vary from 65 to 80 percent and 32 to 14 percent from the base to the flow top.

Actinolite apparently replaced the original ferromagnesian mineral(s) and mafic glass, and forms a poikiloblastic polycrystalline matrix. The actinolite occurs in several habits including equant to elongated, anhedral to locally subhedral grains (0.2mm average size), finely radiating acicular needles (0.2mm long), and coarser bladed prisms (up to 1mm long).

Equant to elongated actinolite grains are ubiquitous throughout all flows. Finely radiating acicular actinolite is generally restricted to the upper and lower parts of some flows, particularly the lower one third of massive flows in areas devoid of plagioclase laths and prisms (Fig. 14). In the lower parts of these flows, actinolite content approaches 70 percent and plagioclase is an inequigranular mosaic interstitial mineral. In some massive flows however, large plagioclase laths and prisms occur in the lower part of the flow and acicular actinolite textures are absent. Such areas may represent a pre-existing very fine granular or glassy material.

Coarser bladed prisms of green to blue-green actinolite form feathery growths that locally overgrow other actinolite. They appear to be the result of more extensive recrystallization and increase in abundance towards the gabbro sill.

Primary plagioclase textures vary systematically throughout many massive flows (Fig. 14), and there are subtle textural differences between adjacent flows. Thus, if the actual flow contact is not exposed, adjacent flows can be distinguished by textural differences.



- 1 quartz-filled amygdules
- 2 local semi-trachytic textures
- 3 local pseudomorphosed subophitic textures with Schiller structure
- 4 equant to elongated granules of actinolite
- 5 feathery intergrowths of acicular actinolite
- 6 areas devoid of large (2mm) plagioclase laths and prisms
- 7 microlitic plagioclase laths
- 8 prisms of corroded plagioclase
- 9 well twinned laths of plagioclase
- 10 microporphyritic and/or clotted plagioclase textures
- 11 swallow-tail and belt-buckle plagioclase morphologies

Figure 14. Composite section depicting the distribution of minerals, primary textures, and primary structures in a typical massive aphyric flow.



Most plagioclase grains have retained their primary shape although they are corroded by actinolite. Primary plagioclase occurs in three distinct morphologies: corroded poorly twinned prisms, well twinned laths and, microlitic twinned laths. Similar plagioclase morphologies were noted in Cenozoic abyssal tholeiites by Aumento et al, (1977).

Corroded prisms range in length from 0.6mm to 1.2mm. They have poor Carlsbad twins (where developed), are partly replaced by acicular actinolite, and are locally bent and broken; in places some grains appear to be parts of larger broken crystals. The bending and breaking is probably due to metamorphism and/or deformation. The prisms are generally confined to the lower two thirds of the flow, but are present throughout some flows (Fig. 14).

Lath-shaped plagioclase grains are ubiquitous and are the most abundant plagioclase morphology. They differ from corroded plagioclase prisms in that the prisms are more equidimensional, usually smaller, less numerous, and more poorly twinned. The laths range in length from 0.2mm to 2.5mm and have well developed albite twins and rarer Carlsbad and Carlsbad-albite twins. Oscillatory zoning is present and the composition is about An_{50} . Some grains are slightly fractured, probably by deformation. In the lower parts of some flows, large laths and prisms of plagioclase are concentrated in clots separated by finely radiating acicular actinolite and produce a clotted texture (Fig. 14).

Microlitic laths of plagioclase are present only in the lower third of some massive flows and are distinguished from laths and prisms by their small size (0.3mm). They may or may not show albite twinning. They occur in conjunction with both well twinned laths and

corroded prisms to form microporphyrritic textures; the laths and prisms are phenocrysts and the microlites are groundmass (Fig. 15). In several flows both clotted and microporphyrritic textures are present, although the two textures do not occur in the same part of the flow. The transition from clotted to microporphyrritic textures occurs both vertically and laterally; in massive flows 9 and 11, the lateral transition from microporphyrritic to clotted textures occurs in a lateral distance of less than 200m.

Microlitic laths increase in size upwards and near the centre of the flow they are indistinguishable from well twinned plagioclase laths.

In the center of several flows of varying thickness, the microlitic laths locally have belt-buckle and swallow-tail shapes (Fig. 16, 17) that are characteristic of rapid quenching of basaltic magma (Bryan, 1972). Because the belt-buckle and swallow-tail shapes are absent in the marginal parts of these flows, they cannot represent simple quenching. However, they may represent rapid cooling of a crystal-poor residual liquid (T. Pearce, personal communication). The belt-buckle and swallow-tail shapes are restricted to 7mm to 10mm thick irregular zones that also contain fine-grained acicular actinolite but lack the larger plagioclase laths and prisms characteristic of adjacent parts of the flow. These irregular zones probably represent areas of crystal-poor residual liquid situated between the more crystallised areas that are abundant in large plagioclase laths and prisms. The irregular zones underwent rapid cooling thus forming the belt-buckle and swallow-tail plagioclase. Selective metamorphic corrosion by actinolite could also have produced



Figure 15. A twinned, corroded and partly fractured plagioclase lath surrounded by smaller, twinned microlitic plagioclase laths. Top picture in plane-polarised light, lower picture with crossed nicols. Field of view 1.2mm x 0.78mm.

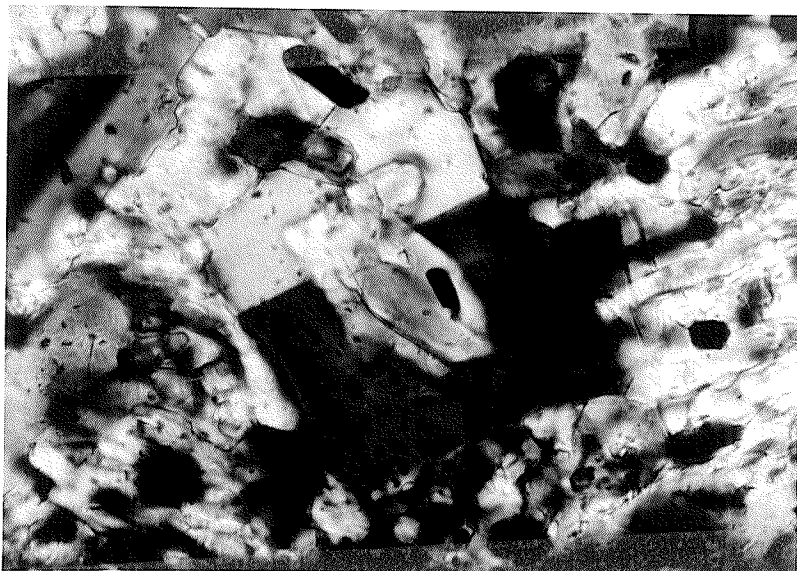


Figure 16. A twinned microlitic plagioclase lath with belt-buckle morphology. Note the iron-titanium oxide granule inside the belt-buckle. Field of view 0.24mm x 0.157mm.



Figure 17. Corroded plagioclase microlite (white) with swallow-tail morphology. Field of view 1.2mm x 0.78mm.

the belt-buckle and swallow-tail morphologies but most of these grain shapes appear to be primary.

Plagioclase grains generally have a felted texture but local semi-trachytic alignment of plagioclase laths was observed in the upper parts of some flows (Fig. 14).

The upper and lower chilled zones contain less than 5 percent corroded plagioclase laths (0.3mm to 0.6mm long) in a very fine mosaic of inequigranular plagioclase and actinolite (0.05mm) that may represent recrystallized very fine-grained granular or glassy primary groundmass. Plagioclase decreases in size (Fig. 6) and abundance near the top and bottom of most flows. Similar decreases in size and abundance of plagioclase have been observed in abyssal tholeiitic basalt from the Mid-Atlantic Ridge (Aumento et al., 1977).

Textures of the original ferromagnesian minerals are preserved only in flow 5 where subophitic actinolite pseudomorphs after pyroxene are locally present in the basal part of the flow. The former presence of pyroxene is indicated by white patches in the center of some actinolite grains. These patches contain oriented trains of fine iron-titanium oxide grains that may represent Schiller structure in the original pyroxene (Fig. 18).

Some evidence of original isogranular and intergranular pyroxene textures has been observed. In most flows, there are places where anhedral actinolite grains become quite large (0.6mm) and occur between two or three larger plagioclase laths (1.2mm to 2.5mm). Actinolite grains near the base of some flows are locally the same size as plagioclase laths (0.3mm) and occur between the laths. In both of these examples the actinolite grains could be pseudomorphs after

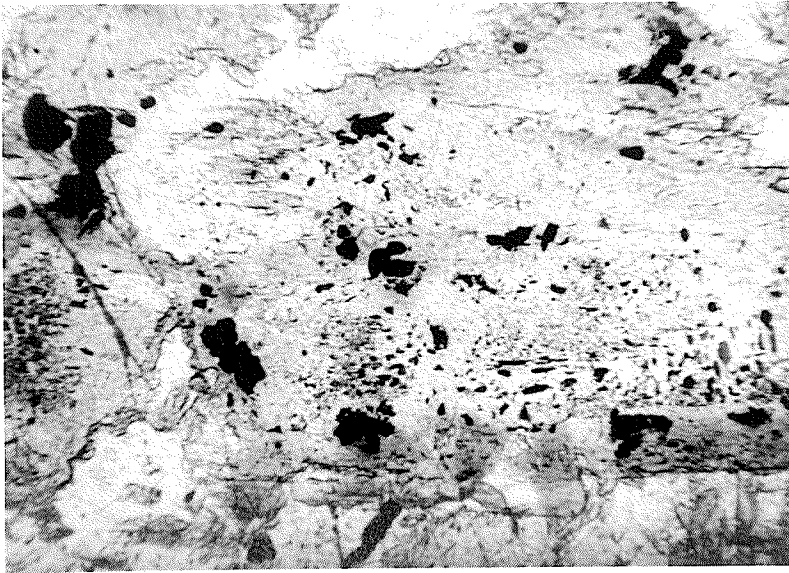


Figure 18. Pale green actinolite grain (light shading) with lighter blotches containing oriented iron-titanium oxide granules that may represent Schiller structure near the base of flow 5. Field of view 1.2mm x 0.78mm.

intergranular and isogranular pyroxene respectively. However, the evidence is inconclusive.

Pearce (1974) has also noted the absence of groundmass pyroxene and olivine in basaltic flows with well preserved primary textures in the Superior Province. These flows as well as those at Utik Lake differ from abyssal tholeiitic basalts of the Mid-Atlantic Ridge and subaerial Hawaiian flows in the absence of olivine and/or pyroxene phenocrysts.

Discordant inequigranular quartz veinlets are locally present in the chilled zones. Secondary plagioclase veinlets are also present in some flows, and like quartz veinlets, are a product of metamorphism.

Pillowed Flows

Introduction

Ellipsoidal pillows of both interconnected and apparently discrete types occur in two main habits: as incipient pillows at the base of some massive flows, and, as pillowed flows.

Incipient pillows that occur in the basal chilled zone of massive flows are genetically related to these flows and were discussed previously.

Most pillows occur in pillowed flows or flow sequences that vary in thickness from 1m (Plate 1, flows 12, 18, and 23) to 100m (flows 2 plus 4, Plate 1).

Pillows vary in size and shape from 10cm spheres to balloon-, bun-, and mattress-like forms that attain cross-sectional lengths of 7m. No size gradation was noted within or between flows except for flow 2 (Plate 2) where pillow size seems to decrease upward.

The thicker pillowed units (20m to 100m) may represent more than

one pillowed flow. Here, the internal flow contacts would be pillows adjacent to pillows with no obvious morphological or textural indicator of the contact. However, possible flow contacts can be defined by the presence of lateral zones of intrapillow cavities, conformable alteration zones, and thin (2cm) zones of hyaloclastite tuff adjacent to pillow selvages.

A subaqueous process similar to the digital advance of subaerial pahoehoe toes (Jones, 1968) probably produced the pillows in the aphyric sequence. Data that support this conclusion include: the irregular and interconnected nature of individual pillows, incompletely formed pillow selvages, and the intrapillow cavities and concentric zoning within pillows.

Petrography of Pillows

The centres of pillows are mineralogically identical to massive flows but are finer grained (0.8mm average grain size). Primary textures are rarely preserved and where present consist of 35 percent, randomly oriented, corroded plagioclase laths that locally have swallow-tail and belt-buckle morphologies in a groundmass of 60 percent actinolite and 5 percent iron-titanium oxide grains. The original glassy selvages now consist of two zones: an outer deep green zone 2cm thick, and an inner black zone 3mm thick. The outer zone is mostly inequigranular actinolite (0.2mm to 2mm long) with minor plagioclase, biotite, sphene, iron-titanium oxide grains and clinozoisite. The inner black zone consists of radiating clusters of acicular actinolite that grades into both the massive inner portion of the pillow and the outer zone.

Recrystallized and slightly flattened variolites up to 6mm long

occur in a 5cm zone immediately below the inner black zone of the selvage of the pillows in the upper part of the sequence. The variolites are now spheroidal intergrowths of plagioclase and acicular actinolite (Fig. 19). In modern pillows, variolites occur immediately below the fresh glass margin of the selvage (Scott and Hajash, 1976), and by analogy, the inner black zone of the selvage may represent the fresh glass margin (tachylite) whereas the outer zone represents the outermost altered glassy rim (sideromelane).

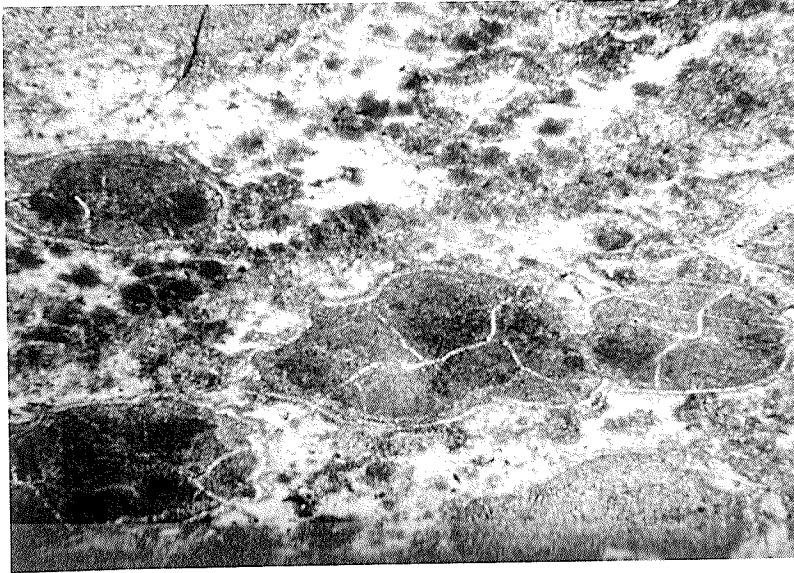
Ovoid amygdules up to 1mm long occur in a 7mm zone immediately below the selvage of some pillows. They consist of equigranular quartz rimmed by bladed actinolite.

Internal and External Structures

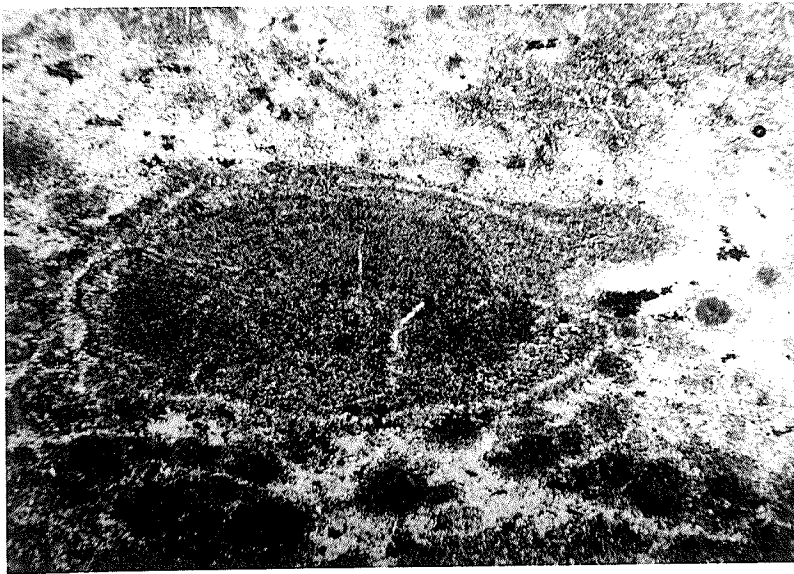
Pillow Selvages

In most pillows, the selvage can be distinguished from the pillow center by its deeper green colour. However, in some pillows the distinguishing colour differences are absent although the selvage has the same textures and mineralogy as darker coloured selvages elsewhere. Superficially, such pillows appear to have incomplete selvages but the colour difference probably reflects differences in alteration. The darker colour of the normal selvage probably reflects initial palagonitisation which is a ubiquitous alteration in most pillows. The absence of the darker colour would thus reflect lack of palagonitisation due to a tight initial seal between two adjacent pillows, which prevented ocean water access.

In some pillows, the selvage continues inside the pillow as a vertically oriented re-entrant selvage (Fig. 20). Such selvages may form when a lava tube or submarine pahoehoe toe bifurcates (Vuagnat,



(a)



(b)

Figure 19. Photomicrographs of variolites near the pillow selvages in pillowed flow 23 in the southwest corner of the area. The variolites are slightly flattened. Field of view (a) 12mm x 7.85mm, and (b) 4.8mm x 3.14mm.

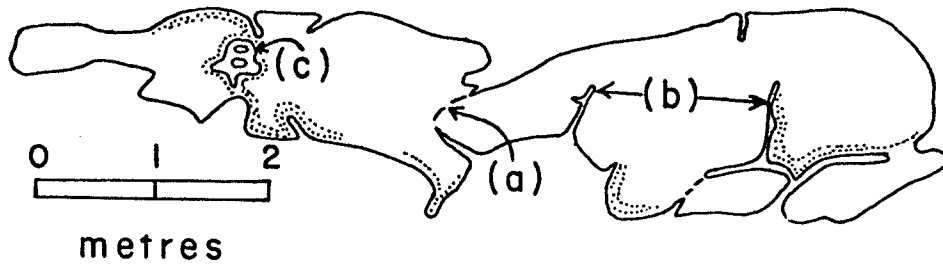


Figure 20. Outcrop diagram of two pillows at the top of pillowed flow 20 (Fig. 5). Pillows show a lateral incomplete selvage (a), deep vertically oriented re-entrant selvages (b), and concentric zoning (dotted) that is partly developed around both normal and re-entrant selvages (c).

1975) or by pillow budding (Moore, 1975). When several re-entrants occur in the same pillow, pillow budding was most likely the cause. Each re-entrant represents the former end of a pillow that was broken by the budding of a new pillow.

Interpillow Voids

Where the selvages of three pillows meet, but are not in complete contact, interpillow voids are present (Fig. 21). Such voids are tricusped in shape, rarely exceed 12cm in maximum dimension, and are filled by medium to coarse-grained inequigranular quartz or calcite.

Hyaloclastite Tuff

Adjacent to interpillow voids the outer 2cm thick zone of the pillow selva is a hyaloclastite tuff. The tuff is in contact with the inner selva zone, and takes the place of the outer zone. Individual clasts vary from 0.3cm to 1.5cm in length, and are sub-rounded to sub-angular polygons. They consist of equant actinolite (0.3mm) in a mosaic plagioclase matrix (0.01mm to 0.05mm). Bladed and diamond-shaped actinolite (0.3mm to 0.5mm) occupies interclast areas and locally contains anhedral sphenes. The tuff probably resulted from the quenching and granulation of the pillow selva.

A similar hyaloclastite layer surrounds the uppermost one or two pillows in some pillowed flows, even where interpillow voids are absent but was not observed in the central parts of flows. The presence of this preserved hyaloclastite tuff in the uppermost pillows denotes a hiatus in volcanism. Although they were not observed in the sequence, the presence of similar zones within the interior of thick pillowed units might be useful in separating successive pillowed flows.



Figure 21. Photograph of a quartz-filled interpillow void. Lens cap for scale (55mm).

Concentric Zoning

Concentric zoning outlined by colour differences between the zones and the pillow interior is present in the outer parts of large discrete and interconnected pillows (>2m) and is locally present throughout smaller (<1m) discrete pillows. Each zone is about 1cm thick and may represent partial crystallization of successive pulses of magma through a subaqueous lava tube (Clifford and McNutt, 1971).

Intrapillow Cavities

Intrapillow cavities that are commonly filled with quartz occur within some pillows. They are concentrated in the upper part of pillows but are always at least 10cm below the selvage (Fig. 22). In a cross-sectional outcrop view, the number of cavities per pillow varies from 1 to 7; where more than four cavities are present, 2 or more of them may occur at the same level in the pillow (Fig. 22a). The uppermost cavities have arched rooves and flat bases whereas the lower cavities have a flat pancake appearance.

Cavity-bearing pillows are nearly always more squat in form (width to length ratio less than 2:1) than non-cavity bearing pillows as in flow 2 (Plate 2), and usually occur in conformable zones at the top of a pillowed unit and as discontinuous, generally conformable zones within some of the thicker flows (flow 2 in Plate 2).

Waters (1960) among others, has described similar cavities and considered that they formed by the concentration of residual gas at the upper interface between the crystallizing rim of the pillow and the molten interior. Gas would collect at the uppermost part of the pillow; the top of the gas accumulation would conform to the curved upper surface of the pillow whereas the base would be relatively flat and



(a)



(b)

Figure 22. Photographs of intrapillow cavities. Note the variation in size. The cavity in (b) is almost 1m long whereas those in (a) are no more than 15cm long and represent the average sized cavity. Lens cap for scale (55mm).

horizontal. The flat bases of such cavities have been used to determine paleohorizons in ancient sequences (Waters, 1960). At Utik Lake they are generally parallel to both the long axes of the pillows and flow contacts. This suggests that the flows were erupted onto topography with a regional slope of less than 10° .

The concentration of residual gas within discrete pillows should produce only a single cavity within each pillow, but several pillows contain more than one cavity. However, if the pillows are interconnected and developed by a process analogous to subaerial pahoehoe budding (Moore, 1975), then each cavity may represent a pulse of lava through the pillow. Cavities produced by pulses of lava through a pillow would develop during short quiescent periods with rising gas being trapped by the crystallizing rim. Subsequent pulses of lava through the pillow would have smaller cross-sectional areas because inward crystallization would decrease the molten and mobile part of the pillow. Thus the cavities, each of which represents another quiescent period would be successively displaced inward.

The concentration of cavity-bearing pillows in the upper part of the flow may reflect the method of lava supply to the flow front. The initial advance may have formed the main pillowed pile rapidly with most pillows in the interior of the flow being only single buds rather than fully interconnected lava tubes. In order for the flow to continue to advance, lava would have to move through the pillows to reach the advancing flow front. A main feeding system of interconnected pillows must develop. The easiest route for lava to move would be along the top of the initial flow because most of the lower pillows would have developed on the sloping front of the flow and probably terminate at the base of the flow. If the feeding system

formed at or near the top of the pillowed pile, then the cavity-bearing pillows may represent this feeding system. If the rate of lava addition was decreasing during the waning stages of eruption, then cavity formation may have been favoured. If the concentration of cavity-bearing pillows at the top of a pillowed flow denotes a decrease in lava addition, then by inference the presence of concordant zones of cavity-bearing pillows within a pillowed unit may indicate a volcanic hiatus or a flow contact between two successive pillowed flows. Such internal conformable zones are not well developed, and generally show a random scattering or clustering in the center of some flows (flow 2 in Plate 2) some of which may represent internal feeding systems rather than flow tops. A well developed internal cavity-bearing pillow zone was noted in flow 16 and is probably a flow contact.

Relationship between Pillows

Two types of pillows are present in the two-dimensional outcrop cross-sections, individual apparently discrete pillows, and interconnected, irregular pillows, although there is a complete gradation between the two types.

Discrete Pillows

Discrete pillows are very simple in form. They are balloon-, loaf-, and mattress-shaped, and usually less than 3m long. In the plane of exposure, these pillows do not have any connection to adjacent pillows, but they are always associated with interconnected pillows. Discrete pillows outnumber interconnected pillows by ratios of 3:1 to as much as 6:1 from flow to flow, but the interconnected pillows are larger and by area occupy 40 percent to more than

75 percent of flows. The constant association of the two pillow types suggests that many, if not all apparently discrete pillows are connected to other pillows in the third dimension rather than being truly discrete pillows. Concentric zoning and multiple cavities are present in some discrete pillows. As previously indicated these features probably reflect multiple pulses of magma through pillows, and their presence in apparently discrete pillows is further evidence that these pillows are actually interconnected.

Interconnected Pillows

Interconnected pillows are irregular in shape. The variable nature of the interconnection to adjacent pillows makes it difficult to define pillow shapes and a selection of irregular, interconnected pillows are shown in Figures 23 to 25.

Connections between pillows vary from narrow necks (Figs. 23a, 24b, 24c, and 24e) to re-entrant selvages with no real neck in which the new pillow is separated from the old pillow by a re-entrant selvage (Figs. 20, 23c, 24a, and 25). The pillows generally propagated laterally (Figs. 24, 25) but locally propagated upward (Fig. 23a) and partly downward (Fig. 25c).

Within the pillowed flows, irregular pillows that are much larger in cross-section than adjacent pillows are found locally. These pillows range in size from a length of 7m and a height of 3m to pillows that have the same thickness as simple massive flows. In flow 10 (Plate 4, in pocket) one such pillow is 20m long and 7m thick, but has normal pillow selvages. These large pillows are commonly connected to smaller pillows and may be part of the main feeding system of the pillowed flow, somewhat analogous to subaerial lava tunnels. Poorly exposed

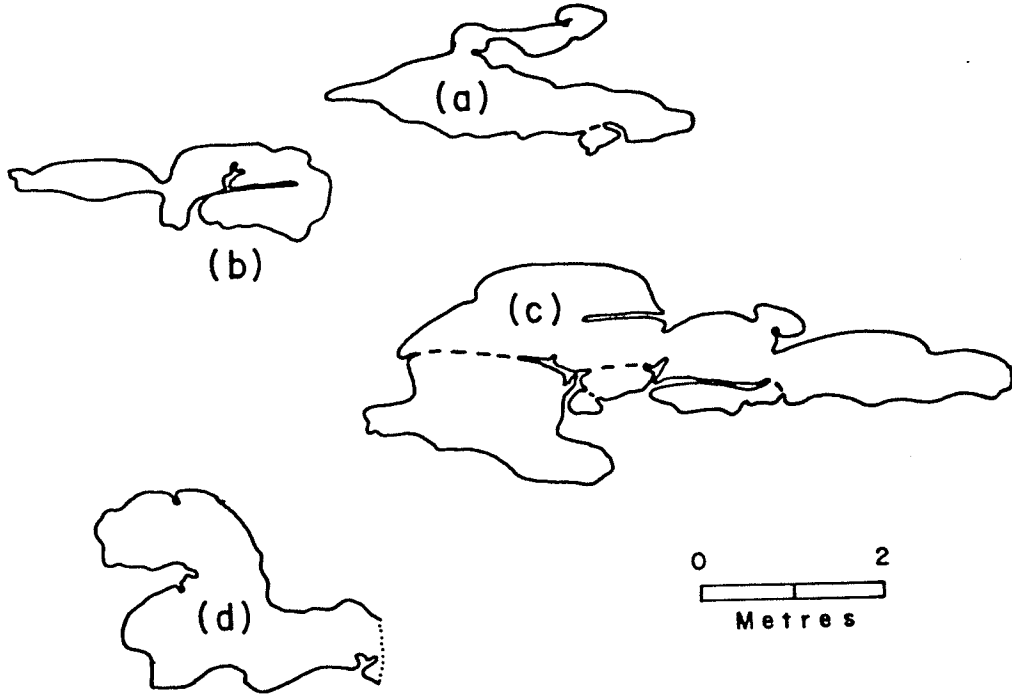


Figure 23. Outcrop sketches of irregular, interconnected pillows.

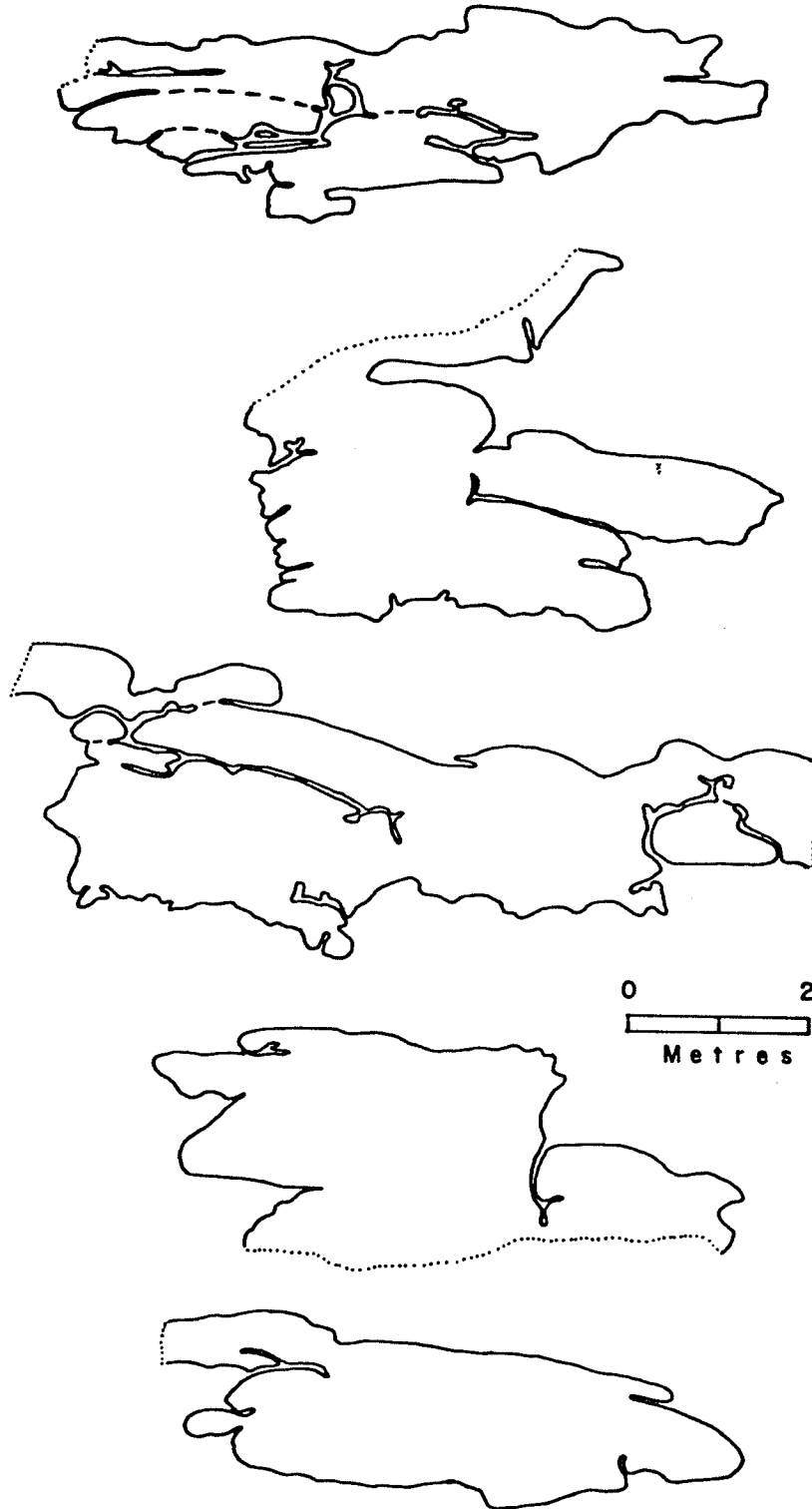


Figure 24. Five examples of larger, irregular, interconnected pillows that probably represent submarine lava tubes. The dashed lines are incomplete selvages whereas the dotted lines are the limit of exposure.

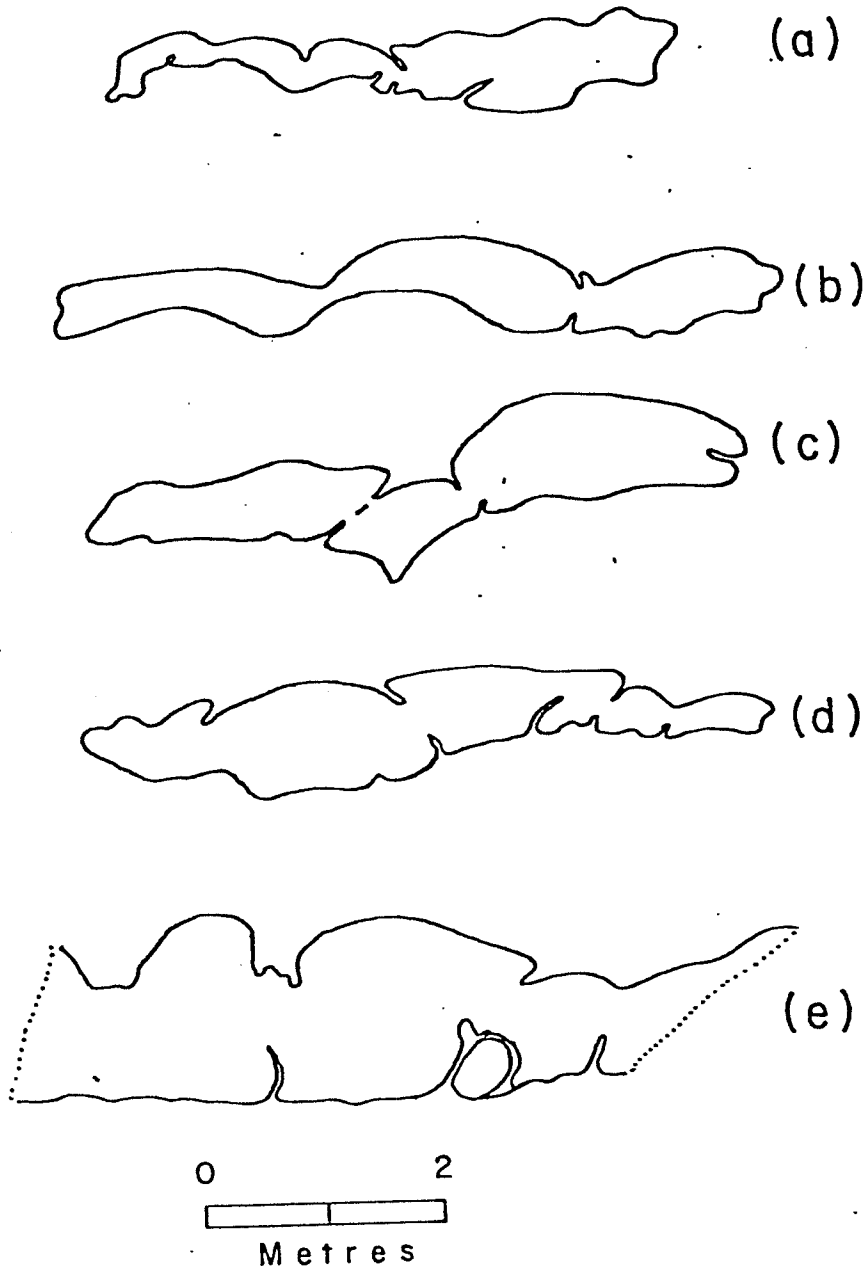


Figure 25. Outcrop sketches of interconnected pillows from various flows. The sketches possibly show longitudinal sections through the pillows showing the nature of their interconnections.

units of this size could readily be misinterpreted as massive flows.

Pillow Alteration

A white to light green weathering alteration composed mainly of fine-grained mosaic diopside is present in some pillows (Fig. 26). The diopside occurs as clots and along fractures in the outer parts of the pillows that do not cross-cut the selvages of pillows in which they are found. Anhedra of epidote (0.5mm), calcite (0.3mm) and laths of clinzoisite (0.2mm in length) are locally found within the diopside. Locally, the alteration occurs between pillow selvages and in places contains anhedral garnet 1mm in size.

Many pillowed flows show no evidence of alteration. However, in those that are altered the alteration is best developed in the upper 2m of the pillowed unit (flow 2, Plate 2). The alteration also occurs within some of the thicker pillowed units: in some units its distribution is apparently random (flow 2, Plate 2), but in other units it is concentrated in concordant zones about 1m thick (flow 4, Plate 2). The alteration probably represents reaction between pillows and ocean water. Such alteration would be most abundant at the top of flows where water ingress is relatively easy. Deeper in the flow where water ingress is more difficult, the alteration would be more sporadic. The conformable, internal alteration zones could represent paths of water ingress, or by analogy with the alteration at the top of the flow, they could represent internal flow contacts. The alteration will be discussed in more detail in a subsequent section.

Origin of Pillows

Although both apparently discrete and interconnected pillows are present in the pillowed flows, most of the pillows probably formed by

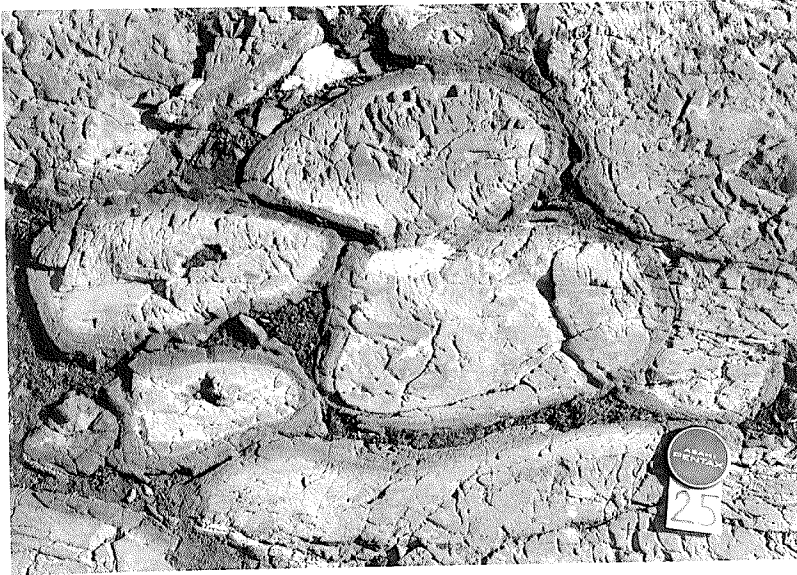


Figure 26. Pillows of flow 4 that contain alteration (light tone).
Lens cap for scale (55mm).

budding and digital advance of subaqueous pahoehoe lava. The discrete pillows probably represent sections across lava tubes rather than true discrete pillows. This mechanism has been observed by Moore et al, (1973) and Moore, (1975) and interconnected pillows have been observed by many workers in both Phanerozoic (Jones, 1968; Vuagnat, 1975) and Precambrian sequences (Côté and Dimroth, 1976). In the Mistuhe Island pillowed flows, digital advance is indicated by the obvious interconnections between some pillows, and the close association between the apparently discrete and interconnected pillows. Intrapillow cavities and concentric zoning in some pillows including both discrete and interconnected types also support this mechanism. Some of the large pillows within the pillowed flows may represent the main feeder channels of the flow.

VOLCANIC STRATIGRAPHY

Introduction

At Mistuhe Island massive and pillowed flows are interlayered with each layer comprising one or more flows of similar aspect (Plate 1). This sequence is similar to many Early Precambrian basaltic sequences and in such sequences it has not always been possible to determine what constitutes a single flow. For example, does each massive and pillowed unit represent a separate flow or is a flow composed of two or more of these units? Do thick pillowed units represent more than one flow? In most of the Mistuhe Island sequence, individual flows were readily defined from a variety of morphologic and petrographic criteria (Table 3). Most massive and pillowed units represent separate flows, but some thick pillowed units appear to represent more than one flow and some massive flows have both massive and pillowed portions.

Criteria for Flow Recognition

Flow contacts can be readily defined by several criteria (Table 3). Massive flows are easier to define than pillowed flows. Most of the criteria are consistent throughout the sequence, and many flow contacts can be defined by several criteria. Basal chilled zones in massive flows, flow-top breccia in complex flows, and smooth surfaces of simple massive flows overlain by flat-based pillows were the criteria most commonly observed. Other criteria such as alteration along subvertical cooling cracks at the top of simple massive flows and thin hyaloclastite zones at the top of massive and pillowed flows are not present in all flows. Alteration at the top of pillowed flows is not always useable because the alteration is not laterally

Table 3. Petrographic and morphologic features used to distinguish individual flows, Mistuhe Island, Utik Lake.

Petrographic textures

- (a) Different primary textures in successive units.
- (b) A very fine-grained granule texture at the top of simple massive flows indicating upward cooling.

Morphologic features

(a) Flow top indicators

Massive flows:

- i) A 1m to 5m thick zone of flow-top breccia in complex massive flows.
- ii) A smooth surface in simple massive flows.
- iii) The presence of alteration along subvertical cracks in simple massive flows that narrow and pinch downward; wider cracks are locally filled by asymmetric pillows from the overlying pillowed unit.
- iv) A thin hyaloclastite zone at the top of some simple massive flows.

Pillowed flows:

- v) Minor hyaloclastite between the uppermost one or two pillows of the flow.
- vi) Concentration of alteration at the top of the flow.
- vii) Concentration of irregular squat pillows that contain one or more quartz-filled intrapillow cavities at the top of a pillowed flow.

(b) Flow base indicators

Massive flows:

- i) A thick (30cm) basal chilled zone with local incipient pillows.
- ii) Primary cooling layers in the basal chilled zone.

Pillowed flows:

- iii) Pillows at the base of pillowed flows that overlie smooth-topped massive flows commonly have flat bases.

continuous (Plate 2).

Thick pillowed units (flows 2 plus 4) posed the greatest problem in defining separate flows. Such units are considerably thicker than other massive and pillowed flows in the sequence and may represent more than one pillowed flow. For such a case, flow contacts would be pillows adjacent to pillows, with no obvious morphologic change to indicate the contact. However, two features that occur at the top of pillowed units also form concordant lateral zones within some pillowed units and may indicate contacts between separate flows. These are intrapillow cavities and alteration zones. Flows 2 plus 4 have a combined thickness of 100m and are the main problem flows. A lenticular massive flow (flow 3, Plate 1) occurs near the centre of this pillowed unit and indicates that at least two pillowed flows are present in this unit, but where the massive flow is absent the flow contact cannot be defined readily because of poor outcrop. However, using the two flow top criteria, flows 2 and 4 each consist of at least three flows that range in thickness from 2m to 30m. Other unrecognized flows may also be present because the internal alteration zones are generally discontinuous, and may be absent. Intrapillow cavity zones coincide with the alteration zones at the top of flow 2, but are not well developed within pillowed flows 2 and 4 (Plate 2). Hyaloclastite zones were not observed within any pillowed flow, but are present at the top of flows 4, 10 and the pillowed portion of flow 20.

The upper surfaces of both simple and complex massive flows are usually flat (flow 19 in Fig. 5; flow 9 in Plate 4) but several flows have slight undulations of up to 1m (flow 21 in Fig. 5, and flow 3 in Plate 2). Pillowed flows also have smooth (flow 10, Plate 4) to

undulating upper surfaces (flow 2, Plate 2). Basal surfaces depend on the pre-existing flow topography (Fig. 27).

Where pillows overlie the flat top of a simple massive flow, basal pillows have flat bases (Fig. 27) indicating that the underlying flow had crystallized at least partly prior to pillow deposition. The base of pillows overlying a flow-top breccia are more rounded and bumpy (Plates 3, 4), with some breccia squeezed upwards between the pillows (Plate 3).

The uppermost pillows in a pillowed flow are not flattened by overlying massive flows, suggesting that the pillows were reasonably hard when the massive flow was erupted.

Lateral Extent of Flows

Flows were correlated from outcrop to outcrop using morphologic and petrographic features. Twenty-six flows were defined (Plate 1) and are numbered in chronological order, but an additional ten flows are probably also present. In the uppermost part of the sequence, the ordering of flows is hindered by the presence of faults, poor outcrop, and the discontinuous nature of flows. For example, flows 17 to 22 are a sequence of simple massive and pillowed flows (Plate 1) but flows occupying the same stratigraphic interval 60m to the west across an overburden covered area are complex flows with flow-top breccia. Whether the flows in these two areas represent separate flows that terminate beneath the overburden or undergo lateral transitions in the same flows from complex to simple massive morphology cannot be determined. Primary textures cannot be used for flow correlation in this area because of strong recrystallization.

Many of the thicker, flat-topped simple and complex massive flows

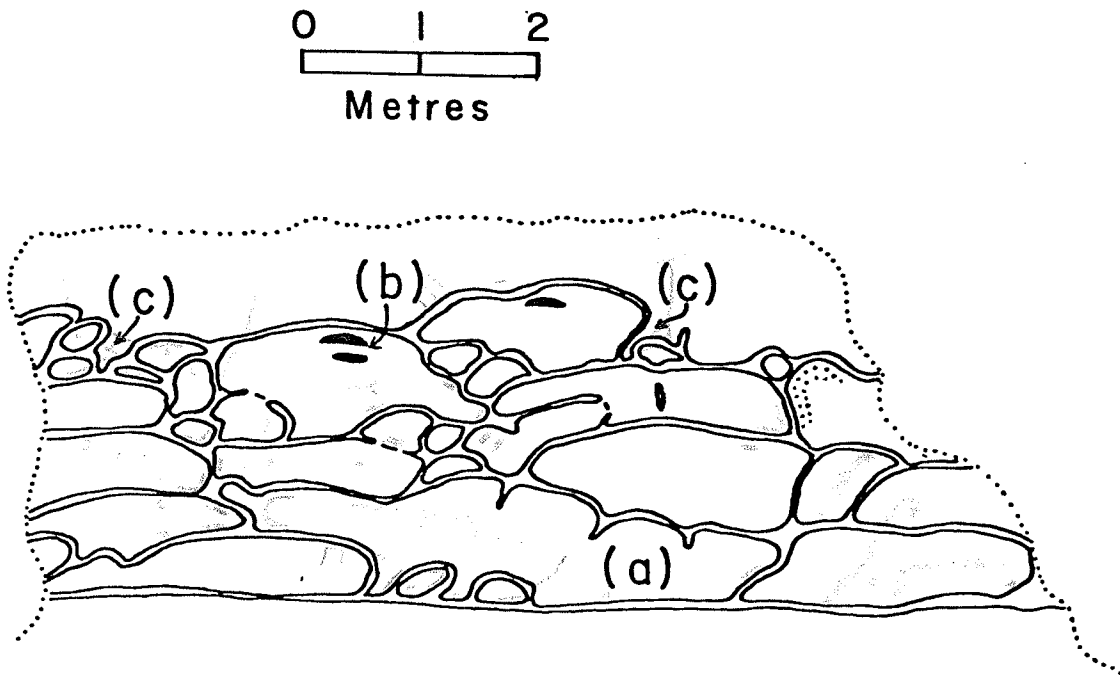


Figure 27. A pillowed flow underlain and overlain by massive flows. The underlying simple massive flow has a flat surface and the basal pillows (a) of the pillowed flow have flat bases. The upper surface of the pillowed flow undulates, and the overlying massive flow has toe-like projections between the pillows (c). Note the intrapillow cavities (b), the concentric zoning (stippled), and the alteration (light green) within pillows and along the base of the overlying massive flow.

have a constant thickness, and extend beyond the map area. They are thus more than 500m long (Plate 1). However, ten massive flows terminate within the map area. Flows 7, 8, 17, 19, 22, and 25 appear to terminate against earlier flows and their terminations are shaped by these flows. Flows 8 and 17 to 20 seem to fill a depression or slope at the top of a pillowed flow. Flows 3, 5, 15, and 24 apparently terminate without being hindered by previous flows. Flows 3 and 22 are lenticular with lengths of less than 80m (Plate 1), and may represent small flows or sections through the margins of more extensive flows.

In complex massive flows 5 and 7 the flow-top breccia thins and disappears in the terminal area. Such flows then resemble simple massive flows. Lateral transitions from complex to simple flows might also occur further away from the terminal area and could explain the apparently conflicting morphology of flows 17 to 22 (Plate 1) with the flows immediately to the west. This process is analogous to subaerial basaltic flows in Hawaii where pahoehoe flows laterally change to aa (Swanson, 1973).

Except for the thick pillowed units, most pillowed flows appear to terminate within the map area. Some flows (flow 20) appear to terminate against irregularities in the underlying flows, whereas others (flows 10 and 14) form mounds that have a lateral extent of about 400m and a maximum thickness of 20m.

In flow 20, a simple massive flow was observed to change laterally into a pillowed flow (Fig. 5). The massive part has a relatively steep flow front from which pillows have budded. The pillowed part continues eastward for 70m and then terminates. The simple massive part apparently changes westward into a complex massive flow (Plate 1).

Similar lateral transitions from massive to pillowed units may occur in other flows, particularly massive flow 3, 5, 7, and 15 that terminate within the map area and are either overlain by pillowed flows or terminate against a pre-existing pillowed flow. Where the pillowed flow overlies the massive flow the two are definitely discrete flows, but in the terminal areas which are not exposed, the basal pillows could be a separate unit that budded from the massive flow (Plate 1). These pillowed units would thus comprise two separate flows. Dimroth et al., (1978) have also described the lateral transition of massive to pillowed units in the Noranda-Rouyn area of Québec.

In subaerial basalt flows a lateral transition has been observed from massive to sheet-like pahoehoe flows through flows composed of pahoehoe toes to aa with increasing viscosity (Swanson, 1973). Subaqueous flows may show an analogous transition from complex to simple massive to pillowed with increasing viscosity or decreasing temperature and flow rate.

A striking feature of the sequence is the interlayered nature of the flow types which may reflect variable viscosity and flow rates from flow to flow. Some pillowed units are a lateral transition from massive flows but most pillowed units appear to be discrete flows, at least in the plane of exposure. The pillowed flows may represent higher viscosities or lower flow rates than the massive flows. If all flows were erupted from the same vent, then the sequences of pillowed flows (flows 2 and 4, Plate 1) may reflect periods when higher viscosity magmas were erupted at reduced rates. However, if not all flows were erupted from the same vent, the pillowed flows may represent a more distant vent than the massive flows. By analogy with

subaerial basaltic magma, viscosity should increase with distance away from the vent. This would cause pillows to form.

CHEMISTRY

Introduction

Samples from sections across three massive flows were analysed chemically. Flows 5 and 11 are complex flows with flow-top breccias whereas flow 19 is a simple massive flow (Plate 1). The sampled sections were completely exposed and very little visible alteration was present. Twenty-four samples were analysed, and the results and norms are listed in Table 4.

When plotted on AFM ternary diagrams the flows are tholeiitic basalt (Fig. 28). The interiors of flows 5 and 11 are similar, but flow 19 contains more K_2O and Na_2O than the other two flows (Plate 5).

Primary Variations

Chemical variations produced by crystal fractionation in mafic magmas can be examined best using MgO variation diagrams (Wright, 1971; 1974). However, for these diagrams to be meaningful, MgO variation of the data should exceed 10 percent of the total weight (Table 4). In the three flows studied, the variation in MgO from flow to flow or within individual flows is less than 3 percent of the total weight (Table 4) which suggests very little fractionation during crystallization of the flows or in the magma chamber from which the flows were erupted. The lack of fractionation is also shown by the slight and generally random variation of major and minor elements when plotted against flow height (Plate 5). The strong variation at the top of flow 5 and 11 reflects alteration in the flow-top breccia. In flow 5, which is the thickest massive flow in the sequence, MgO and Ni increase and CaO decrease slightly in one sample near the base of the flow. This may reflect local fractionation of pyroxene or possibly

Table 4. Chemical analyses and Barth-Niggli norms of samples from massive flows 5, 11 and 19. $\text{FeO}_T = \text{FeO} + 0.8998 \text{Fe}_2\text{O}_3$. Normative values calculated using a computer program established by Irvine and Baragar (1971) that corrects for excessive oxidation of iron. Chief chemical analyst, K. Ramlal.

Sample	SiO_2	Al_2O_3	Fe_2O_3	FeO	FeO_T	MgO	CaO	Na_2O	K_2O	H_2O	CO_2	TiO_2	P_2O_5	MnO	S	Ni(ppm)	Cu(ppm)	Co(ppm)	Zn(ppm)	Total(%)
5-1	49.45	14.98	1.35	9.32	10.53	8.40	11.48	1.76	0.08	1.39	0.08	0.70	0.10	0.21	0.110	196	111	62	69	99.16
5-2	49.90	14.82	1.86	9.22	10.89	8.60	10.88	1.82	0.19	1.52	0.09	0.82	0.14	0.21	0.089	186	105	59	74	99.96
5-3	50.15	15.02	1.28	9.42	10.57	9.20	10.76	1.36	0.10	1.56	0.14	0.78	0.10	0.20	0.160	226	127	58	67	100.10
5-4	50.75	14.80	2.59	8.28	10.61	7.90	10.98	1.94	0.05	1.46	0.05	0.76	0.12	0.19	0.092	151	111	44	66	99.70
5-5	50.45	15.20	2.37	8.48	10.61	7.50	11.56	1.54	0.09	1.56	0.13	0.74	0.12	0.20	0.123	142	111	51	75	99.82
5-6	49.50	15.36	2.36	8.28	10.40	8.00	11.88	1.96	0.08	1.38	0.10	0.72	0.15	0.19	0.107	164	113	56	67	99.83
5-7	49.60	14.96	2.24	8.36	10.38	8.40	11.78	1.68	0.06	1.53	0.06	0.74	0.14	0.21	0.061	193	95	52	71	99.60
5-8	49.60	14.98	2.08	8.56	10.43	8.40	11.68	1.76	0.06	1.54	0.08	0.74	0.12	0.21	0.065	147	93	48	71	99.66
5-9	50.50	15.21	2.02	8.58	10.40	7.70	11.74	2.32	0.06	1.43	0.18	0.74	0.30	0.20	0.135	182	104	51	70	100.91
5-10	49.40	12.69	2.25	6.50	8.52	7.40	18.80	1.08	0.12	1.44	0.14	0.52	0.09	0.37	0.011	128	38	43	55	100.58
11-1	50.05	14.88	1.40	8.84	10.10	6.90	13.04	1.82	0.07	1.42	0.18	0.70	0.13	0.23	0.118	152	118	59	76	99.64
11-2	48.25	14.70	1.29	8.92	10.08	8.50	11.70	2.12	0.18	1.53	1.78	0.72	0.11	0.22	0.022	167	106	58	68	99.91
11-3	49.75	15.62	1.77	8.64	10.23	8.30	11.22	1.84	0.08	1.48	0.18	0.69	0.08	0.20	0.134	175	108	65	66	99.80
11-4	49.00	16.00	1.60	9.24	10.68	8.30	11.76	1.92	0.10	1.34	0.76	0.72	0.09	0.21	0.049	151	129	59	70	100.93
11-5	49.60	15.22	1.89	8.92	10.62	8.30	11.84	1.50	0.06	1.39	0.13	0.66	0.10	0.22	0.092	146	112	55	69	99.70
11-6	49.50	15.40	1.83	8.94	10.59	8.20	11.86	1.84	0.08	1.38	0.09	0.66	0.14	0.21	0.055	141	103	62	71	100.00
11-7	50.00	14.98	1.63	8.52	9.99	7.50	12.02	2.52	0.20	1.35	0.06	0.74	0.15	0.20	0.039	141	108	43	68	99.75
11-8	48.80	15.60	1.04	6.16	7.10	4.60	18.40	2.24	0.04	1.46	0.19	0.71	0.11	0.38	0.118	133	31	53	66	99.75
11-9	44.00	14.21	2.71	10.22	12.66	7.60	16.40	1.06	0.46	1.64	0.08	0.70	0.09	0.46	0.035	160	66	52	96	99.40
19-1	51.05	15.00	1.96	8.44	10.20	7.00	11.14	2.40	0.22	1.36	0.06	0.78	0.15	0.20	0.033	132	98	57	74	99.59
19-2	51.00	14.82	2.46	8.40	10.61	7.60	11.08	2.30	0.11	1.24	0.09	0.74	0.11	0.21	0.063	141	83	65	75	99.97
19-3	51.55	14.95	2.03	8.34	10.17	7.00	10.78	2.30	0.08	1.24	0.07	0.79	0.13	0.21	0.067	135	86	48	66	99.34
19-4	52.50	14.51	1.46	8.64	9.95	6.90	10.66	2.20	0.17	1.35	0.04	0.79	0.11	0.19	0.065	120	85	47	71	99.44
19-5	51.90	14.59	2.20	8.64	10.62	6.40	11.86	2.02	0.24	1.29	0.04	0.74	0.12	0.23	0.015	131	80	48	72	100.06

Sample	Q	OR	AB	AN	NE	DI	HE	EN	FS	FO	FA	WO	MT	IL	AP	PO
5-1	0.40	0.48	15.21	33.60	0.00	12.58	6.76	17.50	9.41	0.00	0.00	0.00	1.45	1.00	0.22	0.39
5-2	1.00	1.15	16.67	32.36	0.00	11.62	5.81	18.41	9.20	0.00	0.00	0.00	1.98	1.17	0.30	0.32
5-3	2.46	0.60	12.46	35.29	0.00	9.96	4.85	20.93	10.20	0.00	0.00	0.00	1.36	1.11	0.21	0.57
5-4	3.18	0.30	17.84	32.30	0.00	12.20	5.95	16.23	7.91	0.00	0.00	0.00	2.42	1.08	0.26	0.32
5-5	4.39	0.55	14.22	35.29	0.00	12.11	6.21	15.24	7.81	0.00	0.00	0.00	2.41	1.06	0.26	0.43
5-6	0.61	0.48	17.94	33.53	0.00	13.92	6.54	15.56	7.32	0.00	0.00	0.00	2.37	1.02	0.32	0.39
5-7	1.75	0.36	15.46	33.93	0.00	13.79	6.23	16.87	7.62	0.00	0.00	0.00	2.40	1.06	0.30	0.21
5-8	1.25	0.36	16.18	33.58	0.00	13.58	6.37	16.94	7.94	0.00	0.00	0.00	2.23	1.06	0.26	0.25
5-9	0.66	0.36	21.02	31.20	0.00	13.63	6.85	14.64	7.35	0.00	0.00	0.00	2.13	1.04	0.63	0.49
5-10	0.48	0.72	9.90	30.06	0.00	36.13	15.56	2.80	1.21	0.00	0.00	0.00	2.16	0.74	0.19	0.04
11-1	1.77	0.43	16.81	33.16	0.00	16.13	9.90	11.53	7.08	0.00	0.00	0.00	1.51	1.00	0.28	0.43
11-2	1.21	0.46	16.87	34.20	0.00	12.86	6.89	17.02	7.10	0.00	0.00	0.00	1.78	0.96	0.19	0.41
11-3	1.06	0.48	16.86	34.84	0.00	11.58	5.58	17.60	8.49	0.00	0.00	0.00	1.89	0.98	0.17	0.46
11-4	0.00	0.60	17.48	35.23	0.00	12.13	6.54	13.34	7.19	2.87	1.54	0.00	1.70	1.02	0.19	0.18
11-5	1.88	0.36	13.80	35.47	0.00	12.76	6.47	17.09	8.66	0.00	0.00	0.00	2.02	0.94	0.21	0.32
11-6	0.15	0.48	16.82	34.15	0.00	13.08	6.80	16.52	8.59	0.00	0.00	0.00	1.95	0.94	0.30	0.21
11-7	0.00	1.20	23.02	29.48	0.00	15.67	8.48	9.37	5.07	2.89	1.56	0.00	1.73	1.05	0.32	0.14
11-8	0.00	0.24	15.60	33.24	3.02	26.05	16.43	0.00	0.00	0.00	0.00	2.63	1.12	1.02	0.24	0.43
11-9	0.00	2.83	2.19	33.93	4.66	23.58	16.42	0.00	0.00	7.50	5.23	0.00	2.39	1.01	0.20	0.14
19-1	1.77	1.33	22.05	30.20	0.00	13.00	7.29	13.28	7.44	0.00	0.00	0.00	2.10	1.11	0.32	0.11
19-2	1.76	0.66	21.02	30.33	0.00	13.13	6.79	14.79	7.64	0.00	0.00	0.00	2.38	1.05	0.23	0.21
19-3	3.94	0.48	21.19	31.03	0.00	11.92	6.47	13.87	7.53	0.00	0.00	0.00	2.18	1.13	0.28	0.25
19-4	4.83	1.03	20.29	30.02	0.00	11.83	7.03	13.65	8.12	0.00	0.00	0.00	1.57	1.13	0.24	0.25
19-5	4.43	1.46	18.59	30.79	0.00	14.11	8.87	11.06	6.95	0.00	0.00	0.00	2.36	1.06	0.26	0.07

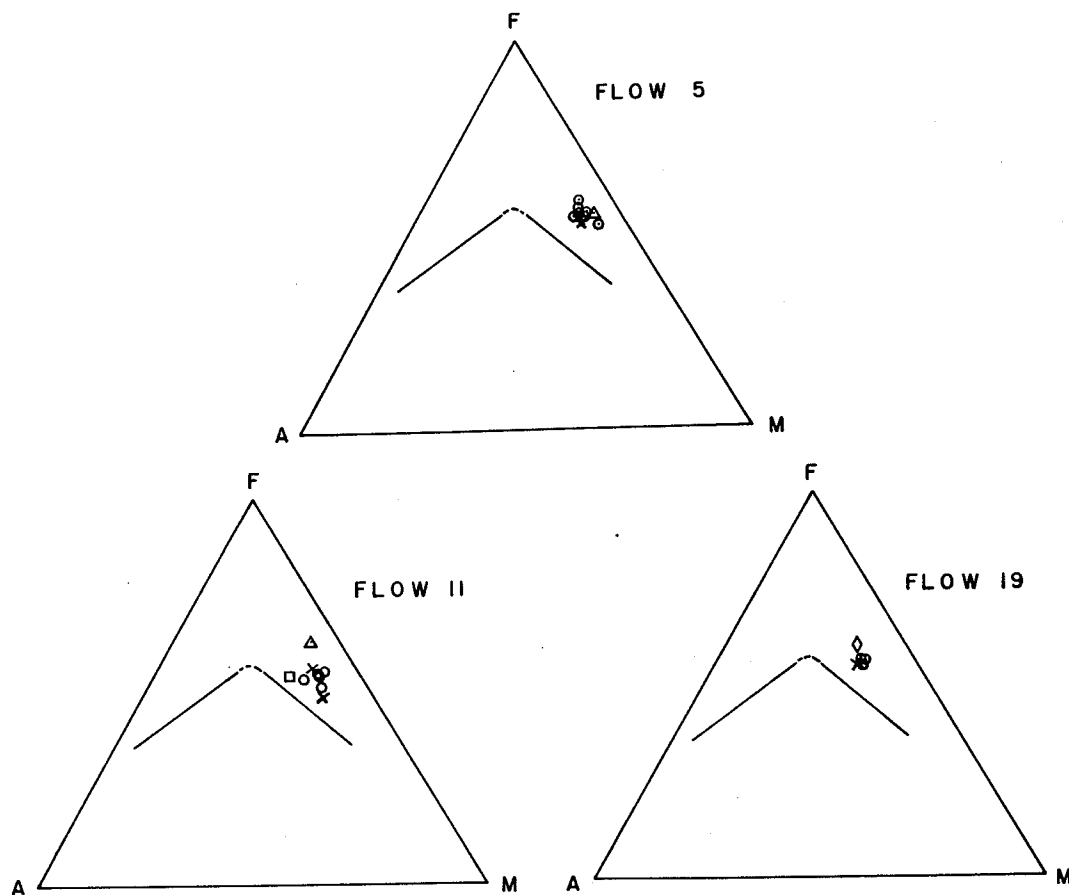


Figure 28. AFM ternary diagrams of complex flows 5 and 11 and simple massive flow 19. The solid line is that of Irvine and Baragar (1971) separating tholeiitic (above) from calc-alkaline fields. Symbols are: x = chilled flow base, o = flow interior, Δ = flow-top breccia matrix, \square = altered massive basalt fragment, and, \diamond = the flow top of simple flow 19.

olivine. Pseudomorphs of pyroxene are found in the lower part of this flow.

Although the chemical variations across the flows do not indicate fractionation, there is considerable scatter in the data, particularly for SiO_2 , Al_2O_3 , FeO_T , MgO and Na_2O (Plate 5). This scatter is probably the result of pre-metamorphism alteration and metamorphic reactions. However, except for the flow-top breccia, which will be discussed later, the nature and magnitude of this alteration is not known.

ALTERATION

If major element analytical error (<0.1 percent) is taken into account, then the scatter in the chemical data (Plate 5) when compared to Hawaiian flows (Moore and Evans, 1966) indicates pervasive alteration is ubiquitous in Mistuhe Island flows. In addition to this, however, a more intense white to light green weathering, diopside-rich alteration is locally present in both massive and pillowed flows.

The chemistry of the alteration has been tentatively determined from three samples from the flow-top breccia of flow 5 and 11 (Plate 5, Table 4). The samples consist of a white weathering massive basalt fragment from flow 11 and a sample of the breccia matrix from each flow consisting of a mixture of dark green basalt lapilli and the altering cement.

Calcium is the most mobile element during alteration, with CaO increasing markedly in both the massive fragment and the breccia matrix (Plate 5). The relatively low CO₂ content of these samples indicates that CaO increase is not due simply to the addition of calcite. Because all oxides in a chemical analysis must sum to 100 percent, the increase in CaO will cause a decrease in all other oxides even though they are not affected by the alteration. Thus in order to determine changes in other oxides caused by alteration, the chemical analyses were recalculated using the average CaO value for the relatively unaltered samples from the interior of the same flow. This recalculation will increase the value of all other oxides, and they can be directly compared to values in relatively unaltered parts of the flow (Table 5). The net gain or loss of the elements is summarised in Figure 29.

Table 5. The mean and standard deviation (σ) of the relatively unaltered samples from the interior of flows 5 and 11. The altered flow-top breccia samples 5-10, 11-9 and 11-8 have been recalculated using the the CaO value of the flow interior. Samples 5-10 and 11-9 represent the breccia matrix whereas sample 11-8 represents an altered white massive basalt fragment.

	FLOW 5			FLOW 11			
	Mean	σ	5-10	Mean	σ	11-9	11-8
SiO ₂	49.99	0.46	53.90	49.35	0.58	46.47	52.80
Al ₂ O ₃	15.04	0.18	13.85	15.32	0.38	15.00	16.88
Fe ₂ O ₃	2.02	0.43	2.45	1.67	0.20	2.86	1.12
FeO	8.72	0.42	7.09	8.86	0.56	10.79	6.66
FeO _T	10.53	0.15	9.30	10.36	0.11	13.37	7.68
MgO	8.23	0.48	8.07	8.18	0.30	8.03	4.98
CaO	11.42	0.40	11.42	11.73	0.22	11.73	11.73
Na ₂ O	1.79	0.26	1.18	1.96	0.31	1.12	2.42
K ₂ O	0.08	0.04	0.13	0.12	0.05	0.49	0.04
H ₂ O	1.48	0.06	1.57	1.41	0.07	1.73	1.58
CO ₂	0.10	0.01	0.15	0.50	0.75	0.08	0.21
TiO ₂	0.75	0.03	0.56	0.70	0.03	0.74	0.77
P ₂ O ₅	0.14	0.06	0.10	0.11	0.05	0.09	0.12
MnO	0.20	0.01	0.40	0.21	0.01	0.49	0.41
Total			<u>100.63</u>			<u>99.34</u>	<u>99.62</u>

Element oxide	Altered sample number		
	5-10	11-9	11-8
SiO ₂	↑↑	↓↓	↑↑
Al ₂ O ₃	↓	-	↑
FeO	↓	↑↑	↓↓
Fe ₂ O ₃	-	↑	↓
FeO _T	↓	↑↑	↓↓
MgO	-	-	↓↓
CaO	↑↑	↑↑	↑↑
Na ₂ O	-	↓	-
K ₂ O	-	↑	-
TiO ₂	-	-	-
P ₂ O ₅	-	-	-
MnO	↑	↑	↑
Ni	-	-	-
Co	-	-	-
Cu	↓↓	↓	↓↓
Zn	-	↑↑	-

Figure 29. Chemical changes during alteration of flow-top breccia. Samples 5-10 and 11-9 represent the breccia matrix whereas sample 11-8 represents an altered white massive basalt fragment. Symbols are: significant gain (↑↑), marginal gain (↑), no gain (-), marginal loss (↓), and significant loss (↓↓).

Some oxides such as CaO and MnO show a consistent increase in all samples, and Cu shows a consistent decrease, but other oxides and elements do not show consistent changes. For example, iron increased in some samples but decreased in other samples. These inconsistent trends probably reflect the variable nature of the breccia. In general, the white weathering massive basalt fragment appears to have more mobile elements than the breccia matrix. TiO_2 , P_2O_5 , Ni and Co appear to be the only immobile elements in the breccia.

Thus, although many elements were mobile during alteration the only consistent changes were a marked increase in CaO, a lesser increase in MnO and a decrease in Cu. The exact mechanism of Ca enrichment is not known, but the marked change between the breccia and the flow interior, and the relatively consistent values in the interior of the flow indicates that it was not leached from the flow interior. The most likely source, considering the location of the alteration at the top of the flow, and its general confinement to the high porosity areas such as the breccias and cracks, is ocean water. This Ca enrichment does not agree with recent work on alteration of Cenozoic pillowed basalts of the Mid-Atlantic Ridge. Scott and Hajash (1976) summarised the findings of many researchers, who found that Ca decreased with increasing pillow alteration. MnO was also noted to increase in the Mistuhe Island sequence. Similar increases were noted during low temperature alteration (halmyrolysis) of Cenozoic pillowed basalts (Hart, 1970; Myashiro *et al*, 1969) but MnO decreased during high temperature alteration (Hajash, 1975; Mottl *et al*, 1974; Bischoff and Dickson, 1975). Cu decreased in Mistuhe Island flows. Similar decreases were observed in experimental hydrothermal alteration by

Hajash (1975) and Bischoff and Dickson (1975).

The addition of Ca and Mn and the decrease of Cu in Mistuhe Island alteration cannot be explained by a single modern day process. Low temperature alteration may account for MnO addition and hydrothermal alteration may account for the decrease in Cu, but CaO addition cannot be explained by modern-day alteration processes. Possibly, Early Precambrian ocean water was different than present day ocean water and this would account for the difference in the behavior of CaO during alteration.

CONCLUSIONS

Thirty-six massive and pillowed aphyric flows were recognized on Mistuhe Island, and are intimately interlayered with each layer comprising one or more flows of similar aspect.

The flows are massive and pillowed and are mineralogically similar. They are composed mostly of primary plagioclase and secondary actinolite. Primary textures are not preserved in all flows, but where present plagioclase forms felted laths and phenocrysts. Primary textures are best preserved in the lower parts of massive flows where plagioclase laths and prisms are associated with microlitic plagioclase forming microporphyritic textures. Microlitic plagioclase have belt-buckle and swallow-tail morphologies in the centres of some massive flows and may have originated by the rapid cooling of a crystal-poor residual liquid.

Except for several of the thicker pillowed units, each massive and pillowed unit represents a separate flow. Individual flows range in thickness from 3m to 35m for massive flows and from 1m to 30m for pillowed flows. Some pillowed units are up to 100m thick but these represent several successive flows. Contacts between these pillowed flows would be pillows adjacent to pillows and flow contacts can be defined only by the presence of lateral zones of intrapillow cavities, and conformable zones of probable ocean-water alteration. Thin zones of hyaloclastite adjacent to pillow selvages were observed at the top of some pillowed flows, but not at the contact between two pillowed flows. However, this could be an additional criteria in other areas.

The upper surfaces of both massive and pillowed flows are usually flat, but some flows have slight undulations of up to 1m. Basal

surfaces in all flows depend upon the pre-existing flow topography.

Many of the thicker massive flows have a constant thickness and extend beyond the map area, a distance of 500m. Other massive flows terminate within the map area either against pre-existing flows or without hindrance from previous flows. A few massive flows are lenticular with lengths of less than 80m and probably represent small flows or sections through the margins of more extensive flows.

In complex massive flows the brecciated flow tops vary in thickness across the map area, and in several flows the breccia is absent near the flow termination. Such flows then resemble simple massive flows and represent a lateral transition from complex to simple massive flows.

Except for the thick pillowed units, most pillowed flows appear to terminate within the map area. Some of these flows apparently terminate against irregularities in the underlying flows, whereas others form mounds that have a lateral extent of about 400m and a maximum thickness of 20m. One simple massive flow was observed to change laterally into a pillowed flow and similar lateral transitions may occur in other flows. In the other direction this flow appears to change to a complex massive flow. The lateral transitions from complex to simple massive to pillowed flows may reflect increasing viscosity or decreasing temperature and flow rate. This transition would thus be analogous to the lateral transitions in subaerial basalt flows from massive sheet-like pahoehoe flow to pahoehoe toes to aa with increasing viscosity.

The massive flows show no evidence of crystal fractionation across flows or between flows. Most major elements show considerable

scatter but this is probably the result of pre-metamorphic alteration and metamorphism.

An intense diopside-epidote-clinozoisite alteration is preferentially developed in flow-top breccias and as clots and fracture fillings in pillows. The alteration involves major addition of Ca, a lesser addition of Mn, and loss of Cu. The exact mechanism of Ca-enrichment is not known, but the general confinement of the alteration to the tops of flows in high porosity areas such as breccias and cracks suggests that the most likely source is ocean water. The Ca-rich alteration in Mistuhe Island flows is dissimilar from Cenozoic ocean-water alteration in that Ca is removed during Cenozoic alteration. This may reflect the difference between Early Precambrian and modern-day ocean water.

REFERENCES

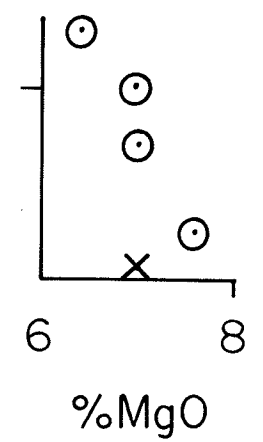
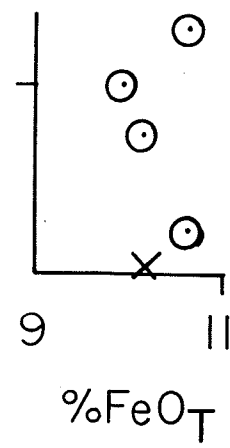
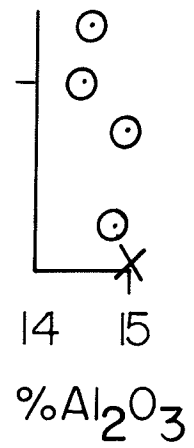
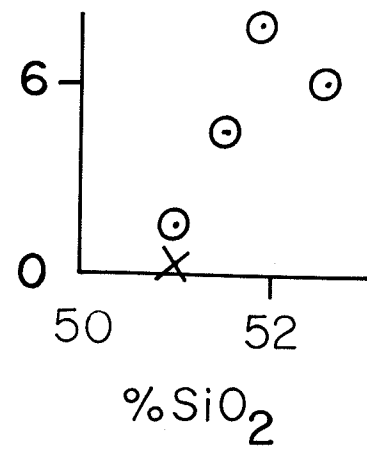
- Allen, C.M., 1953, Geology of the Western Bear Lake area, Manitoba: Dept. Mines Nat. Res., Manitoba, Pub. 52-4.
- Aumento, F., Melson, W.G., Hall, J.M., Bougault, H., Dmitriev, L., Fischer, J.F., Flower, M., Howe, R.C., Hyndman, R.D., Miles, G.A., Robinson, P.T., and Wright, T.L., 1977, Site 332, D.S.D.P. Leg 37. *in* Aumento, F., Melson, W.G., et al., Initial reports of the Deep Sea Drilling Project, vol. 37; Washington (U.S. Govt. Printing Office) p.15-201.
- Baragar, W.R.A., 1968, Major-element geochemistry of the Noranda volcanic belt, Quebec-Ontario: Can. Jour. Earth Sci., v.5, p.773-790.
- Bischoff, J.L., and Dickson, F.W., 1975, Sea water-basalt interaction at 200°C and 500 bars: implications for origin of sea floor heavy-metal deposits and regulation of sea water chemistry: Earth Planet. Sci. Letters, v.25, p.385-387.
- Boutcher, S.M.A., Edhorn, A.S., and Moorhouse, W.W., 1966, Archean conglomerates and lithic sandstones of Lake Timiskaming, Ontario: Proc. Geol. Assoc. Canada, v.17, p.21-42.
- Bryan, W.B., 1972, Morphology of quench crystals in submarine basalts: Jour. Geophys. Res., v.77, p.5812-5819.
- Clifford, P.M., and McNutt, R.H., 1971, Evolution of the Mt. St. Joseph-an Archean volcano: Can. Jour. Earth Sci., v.8, p.152.
- Cole, G.A.J., and Gregory, J.W., 1890, The variolitic rocks of Mont Genève: Quart. Jour. Geol. Soc. London, v.46, p.295-332.
- Cook, H.C., James, W.F., and Mawdsley, J.B., 1931, Geology and ore deposits of the Rouyn-Harricana Region, Quebec: Canada Dept. Mines Geol. Survey Mem. 166, 314p.
- Côté, R., and Dimroth, E., 1976, Flow direction of Archean basalts determined from imbricated pillow breccias: Neu Jahrbuch für Mineralogie. Monatshefte H.3, p.97-109.
- Dimroth, E., Cousineau, P., Leduc, M., and Sanschagrin, Y., 1978, Structure and organisation of Archean subaqueous basalt flows, Rouyn-Noranda area, Quebec, Canada: Can. Jour. Earth Sci., v.15, p.902-918.
- Gelinas, L., and Brooks, C., 1974, Archean quench texture tholeiites: Can. Jour. Earth Sci., v.11, p.324-341.
- Goodwin, A.M., 1962, Structure, stratigraphy, and origin of iron formations, Michipicoten area, Algoma district, Ontario, Canada: Geol. Soc. Am. Bull., v.73, p.561-586.

- Goodwin, A.M., 1966, The relationship of mineralization to stratigraphy in the Michipicoten area, Ontario, p.57-73 in Goodwin, A.M., (ed.) The relationship of mineralization to Precambrian stratigraphy in certain mining areas of Ontario and Quebec. Geol. Assoc. Canada Sp. Pap. 3, 144p.
- , 1968a, Evolution of the Canadian Shield; Proc. Geol. Assoc. Canada, v.19, p.1-14.
- , 1968b, Archean protocontinental growth and early crustal history of the Canadian Shield; Proc. Intl. Geol. Cong., 23rd, Prague, v.1, p.69-89.
- Hargreaves, R., 1974, Volcanic stratigraphy at Utik Lake. In Centre for Precambrian Studies, University of Manitoba, 1974 Annual Report, Part 2-Research, p.128-131.
- , 1975a, Volcanic stratigraphy at Utik Lake. In Summary of Geological Fieldwork, 1975, Manitoba Dept. Mines, Res. and Environmental Management, Mineral Res. Div., Geol. Pap. 2/75 p.26-29
- , 1975b, Basalt flow morphology at Utik Lake, Manitoba. In Centre for Precambrian Studies, University of Manitoba, 1975 Annual Report, Part 2 - Research, p.125-132.
- , 1976, Early Precambrian basalt flows, Utik Lake, Manitoba. In Centre for Precambrian Studies, University of Manitoba, 1976 Annual Report, Part 2 - Research, p.52-55.
- Hart, R., 1970, Chemical exchange between sea water and deep ocean basalts: Earth Planet. Sci. Letters, v.9, p.269-279.
- Hajash, A., 1975, Hydrothermal processes along mid-ocean ridges: an experimental investigation: Contr. Min. Pet., v.53, p.205-226.
- Irvine, T.N., and Baragar, W.R.A., 1971, A guide to the chemical classification of the common volcanic rocks: Can. Jour. Earth Sci., v.8, p.523-545.
- Johnston, W.G.Q., 1969, Pillow lava and pahoehoe: a discussion: Jour. Geol., v.77, p.730-732.
- Jones, J.G., 1968, Pillow lava and pahoehoe: Jour. Geol., v.76, p.485-488.
- Lewis, J.V., 1914, Origin of pillowed lavas: Geol. Soc. Am. Bull., v.25, p.591-654.
- Macdonald, G.A., 1967, Forms and structures of extrusive basaltic rocks: Basalts-The Poldervaart treatise on rocks of basaltic composition. Wiley-Interscience Publishers, New York, v.1, p.1-61.

- Milligan, G.C., 1952, Geology of the Utik Lake-Bear Lake area: Dept. Mines Nat. Res., Manitoba, Pub. 51-4.
- , and Take, W.F., 1954, Eastern Bear Lake area: Dept. Mines Nat. Res., Manitoba, Pub. 53-1.
- Moore, J.G., 1975, Mechanisms of formation of pillow lava: Am. Scientist, v.63, p.269-277.
- , and Evans, B.W., 1966, Olivine in the prehistoric Makaopuhi tholeiitic Lava Lake, Hawaii: Contr.Min. Pet., v.15, p.207.
- , Phillips, R.L., Grigg, R.W., Peterson, D.W., and Swanson, D.A., 1973, Flow of lava into the sea 1969-1971, Kilauea Volcano, Hawaii: Geol. Soc. Am. Bull., v.84, p.537-546.
- Mottl, M.J., Corr, R.F., and Holland, H.D., 1974, Chemical exchange between sea water and mid-ocean ridge basalt during hydrothermal alteration: an experimental study: Geol. Soc. Am. Abst., with Programs, v.6, p.879.
- Myashiro, A.F., Shido, F., and Ewing, M., 1969, Diversity and origin of abyssal tholeiite from the Mid-Atlantic Ridge near 24° and 30° North Latitude: Contr. Min. Pet., v.23, p.38-52.
- Pearce, T.H., 1974, Quench plagioclase from some Archean basalts: Can. Jour. Earth Sci., v.11, p.715-719.
- , and Birkett, T.C., 1974, Archean metavolcanic rocks from Thackery Township, Ontario: Can. Mineral., v.12, p.509-519.
- Pyke, D.R., Naldrett, A.J., and Eckstrand, O.R., 1973, Archean ultramafic flows in Munroe Township, Ontario: Geol. Soc. Am. Bull., v.84, p.955-978.
- Quinn, R.L., 1955, Knee Lake, Manitoba: Geol. Surv. Canada, Paper 55-8.
- Scott, R.B., and Hajash, A., 1976, Initial submarine alteration of basaltic pillow lavas: a microprobe study: Am. Jour. Sci., v.276, p.480-501.
- Swanson, D.A., 1973, Pahoehoe flows from the 1969-1971 Mauna Ulu eruption, Kilauea Volcano, Hawaii: Geol. Soc. Am. Bull., v.84, p.615-626.
- Vuagnat, M., 1975, Pillow lava flows: Isolated sacks or connected tubes? Bull. Volc., v.39, no.4, p.581-589.
- Waters, A.C., 1960, Determining direction of flow in basalts: Am. Jour. Sci., v.258-A, p.350-366.
- Weber, W., 1974a, Utik Lake-Bear Lake Project, in Summary of Geol. Fieldwork, 1974: Manitoba Dept. Mines, Res., Envir. Manag., Min. Res. Div., Geol. Paper 2/74 p.27-32.

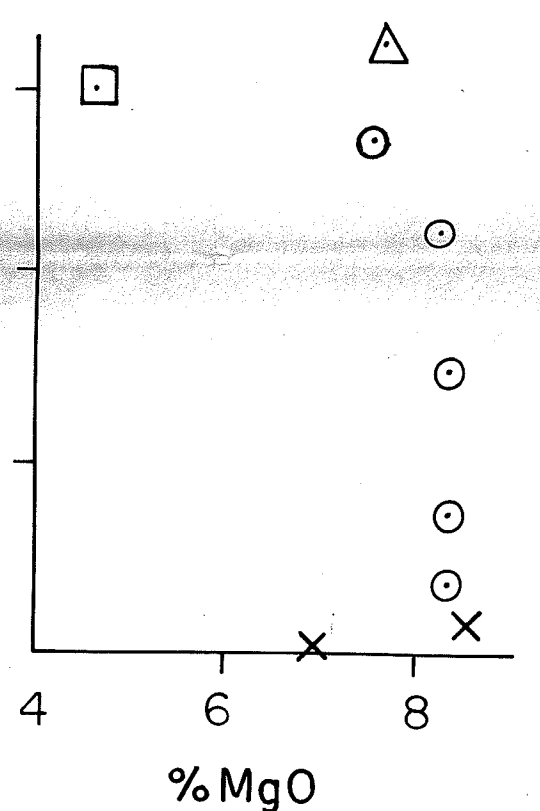
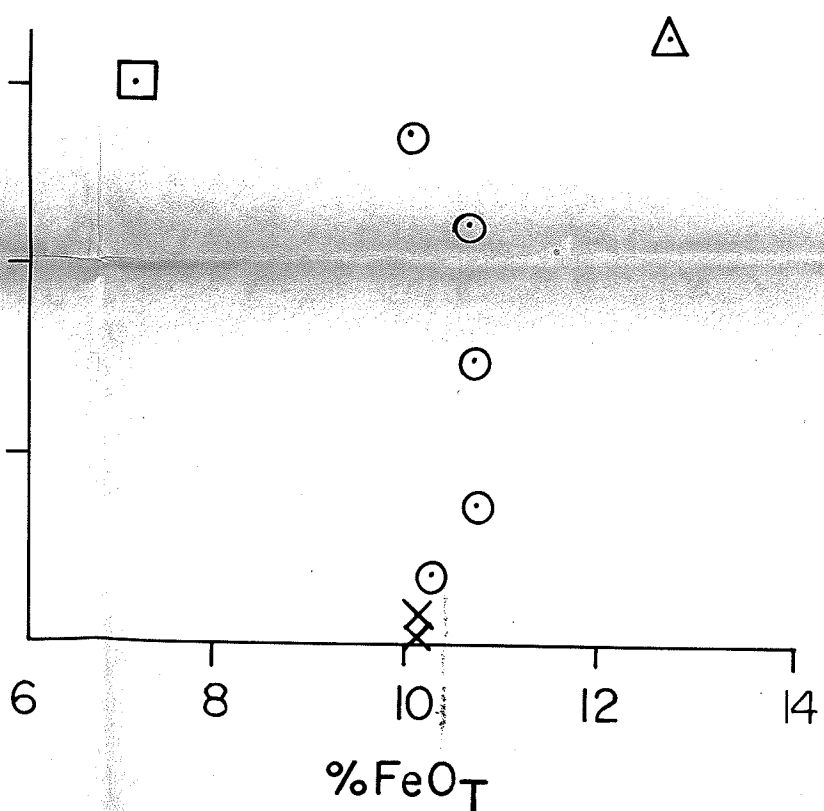
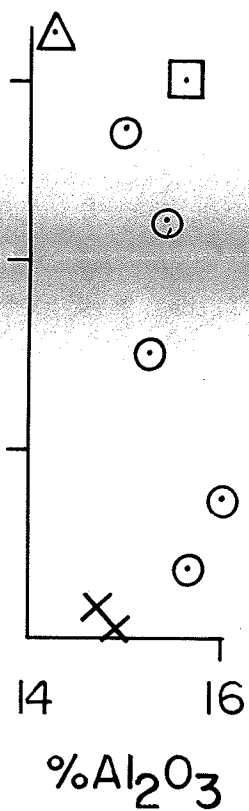
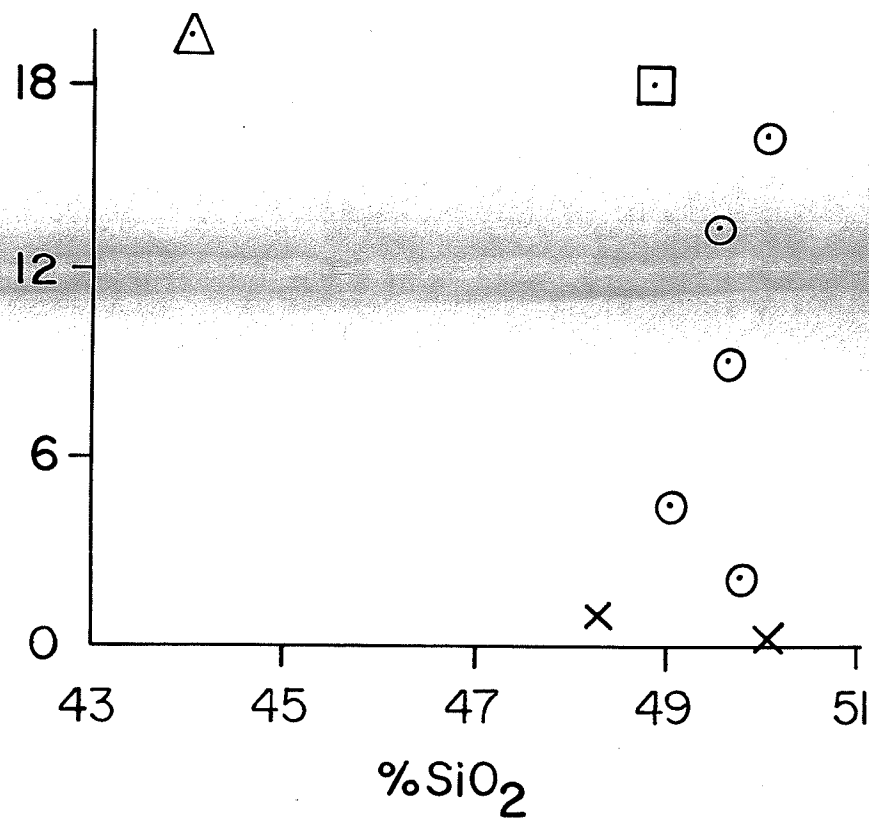
- Weber, W., 1974b, Albright Lake: Man. Min. Res. Div. Prelim. Map 1974U-4.
- Wilson, H.D.B., Morrice, M.G., and Ziehlke, D.V., 1974, Archean continents. Geoscience Canada, v.1, no.3, p.12-20.
- Wilson, M.E., 1942, Structural features of the Keewatin volcanic rocks of western Quebec: Geol. Soc. Am. Bull., v.53, p.53-69.
- Wright, J.F., 1925, Oxford and Knee Lakes area, Northern Manitoba: Geol. Surv. Canada, Summ. Rept., 1925.
- Wright, T.L., 1971, Chemistry of Kilauea and Mauna Loa lava in space and time: U.S.G.S. Prof. Pap. 735.
- , 1974, Presentation and interpretation of chemical data for igneous rocks: Contr. Min. Pet., v.48, p.233-248.

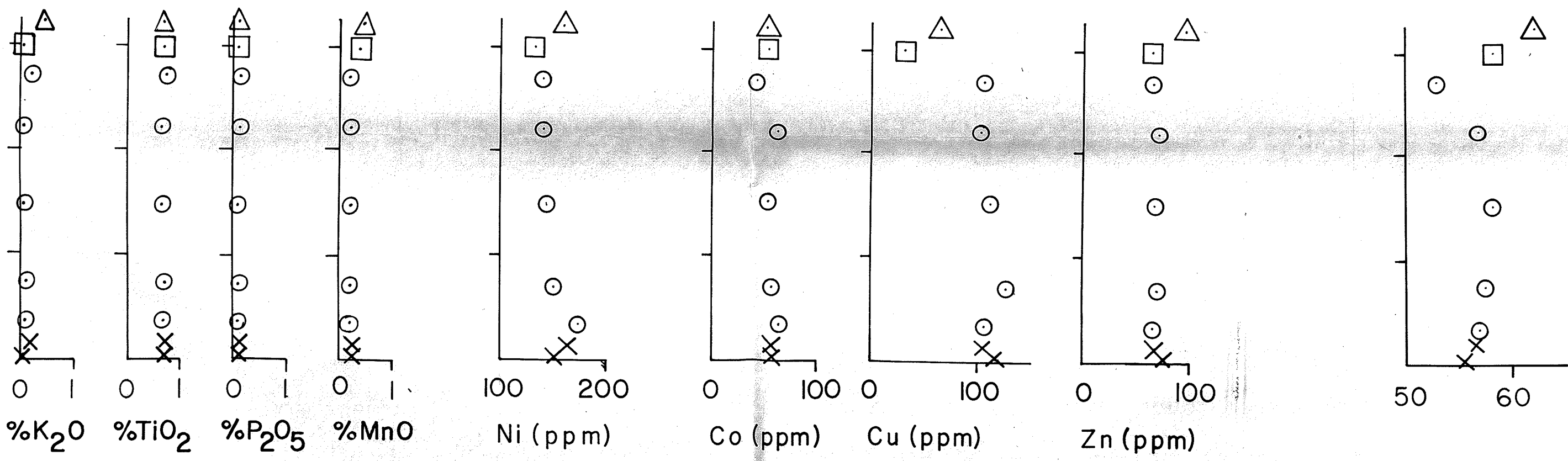
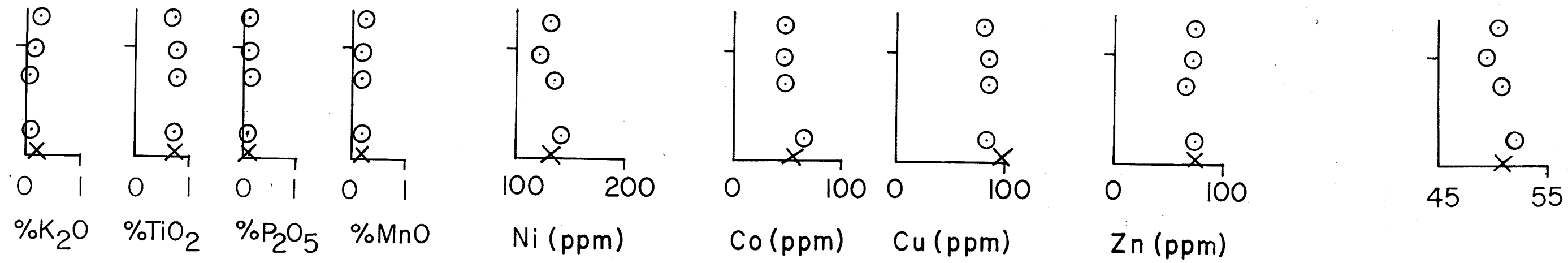
FLOW 19



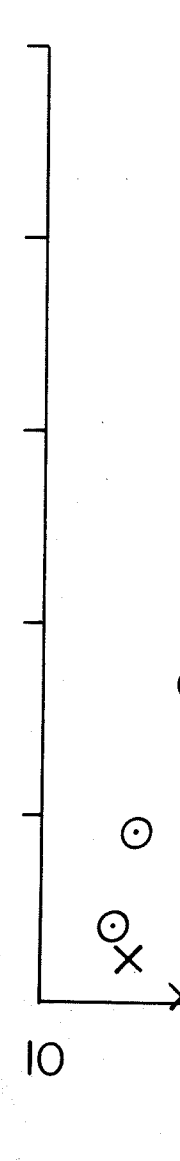
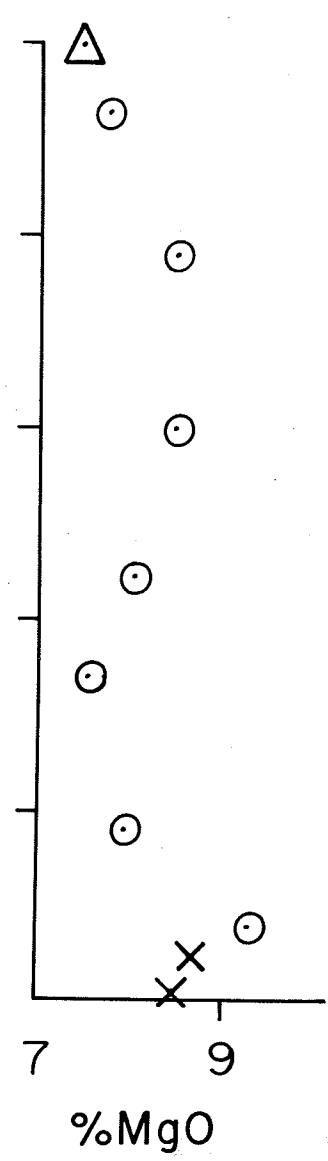
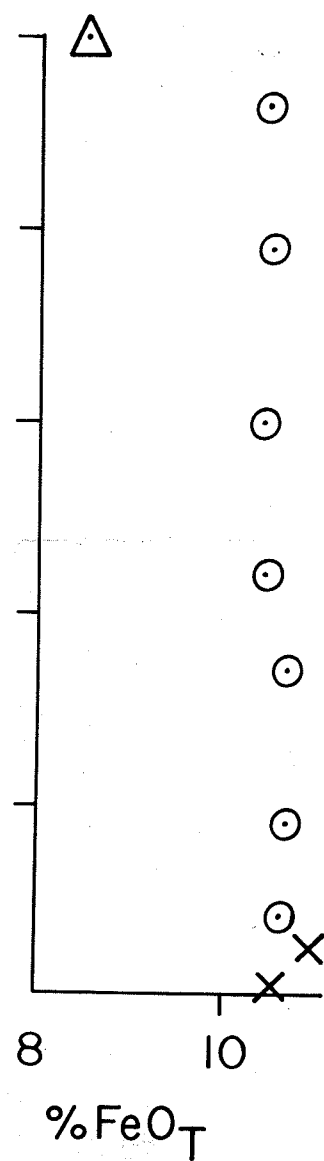
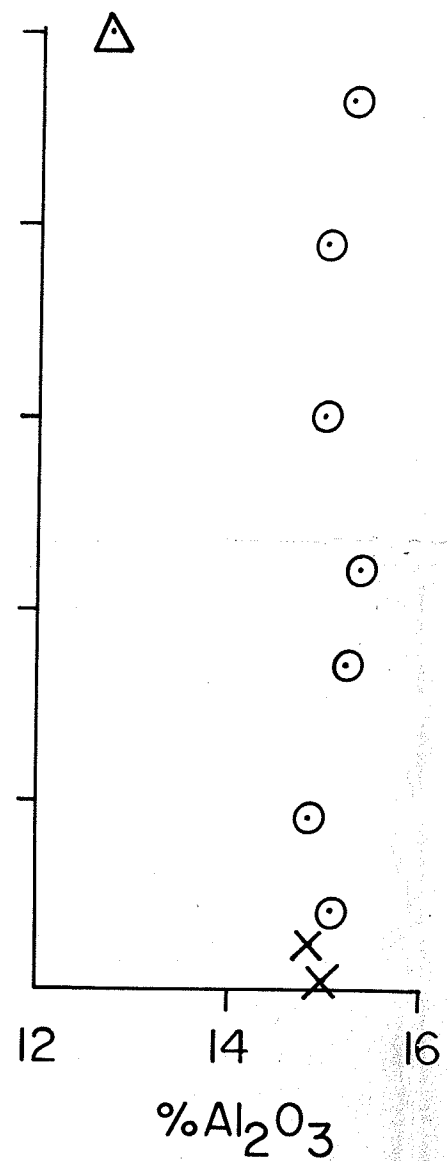
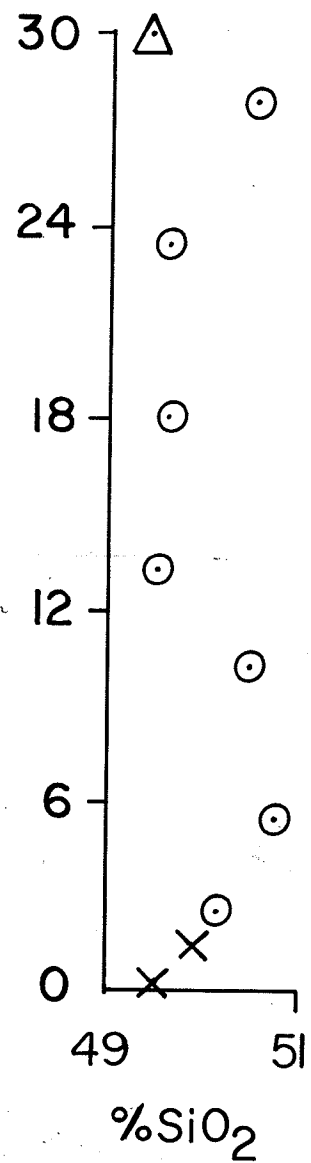
THICKNESS (METRES)

FLOW 11





FLOW



FLOW 5

Plate 5. Thickness versus the major element, minor element and Crystallization Index (C.I.) variation in basalt fragment (□) in the flow-top breccia.



%MgO

%CaO

%Na₂O

%K₂O

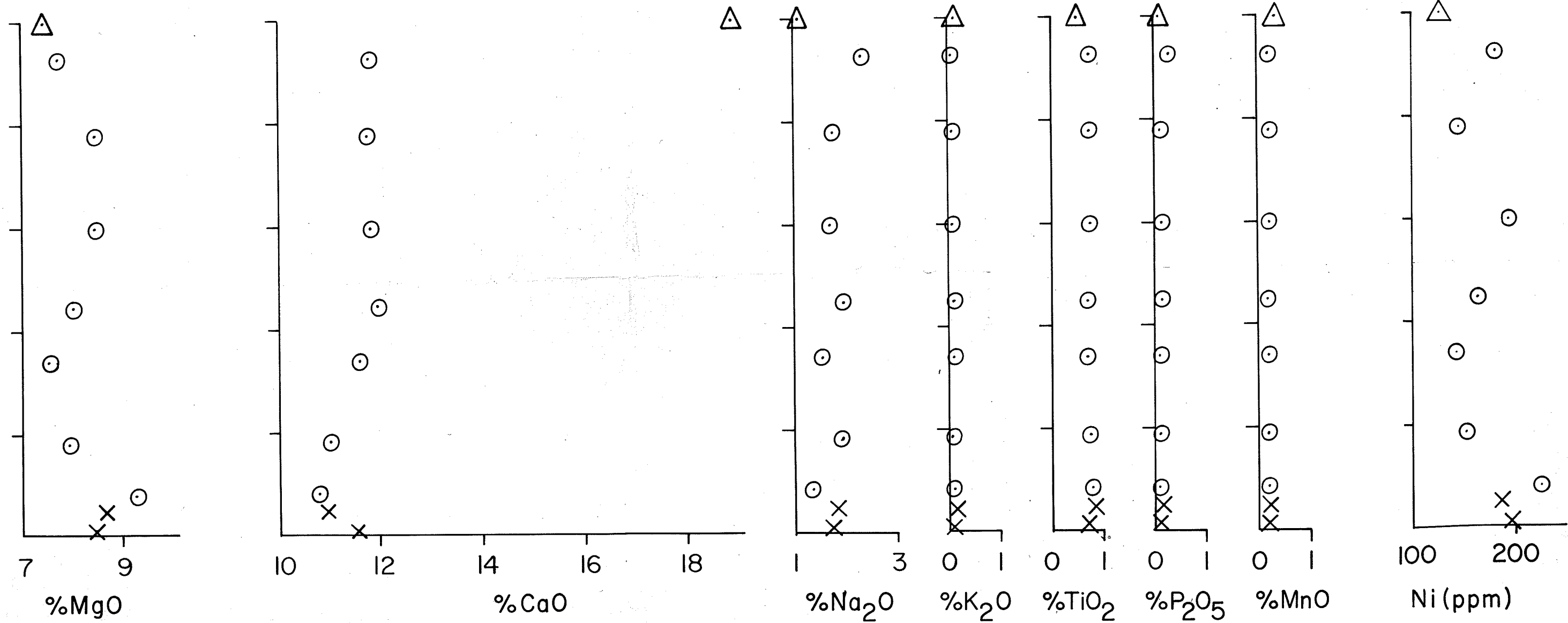
%TiO₂

%P₂O₅

%MnO

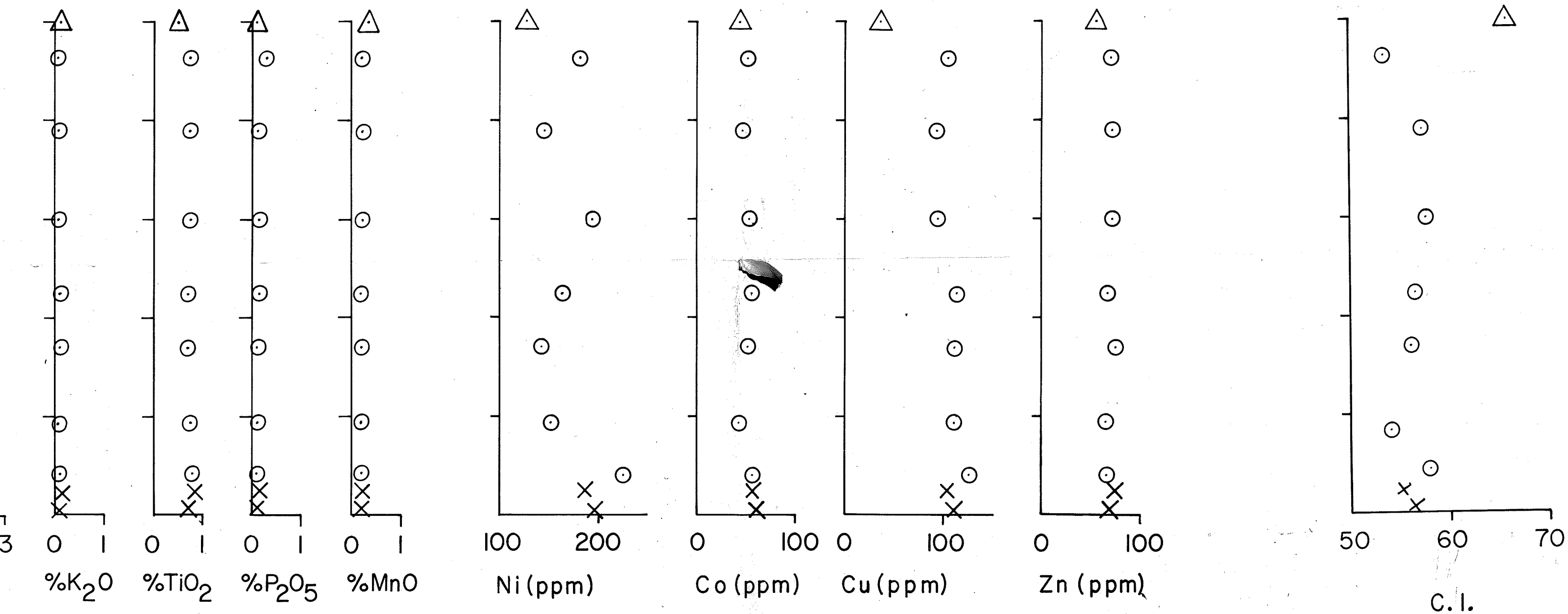
Ni (ppm)

FLOW 5

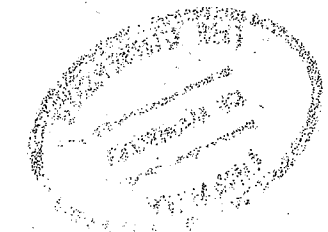


Crystallization Index (C.I.) variation in flows 5, 11, and 19. Symbols represent samples from the flow base (x), flow interior (o)

%K₂O %TiO₂ %P₂O₅ %MnO Ni (ppm) Co (ppm) Cu (ppm) Zn (ppm)




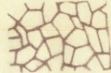
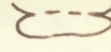

nt samples from the flow base (x), flow interior (⊙), flow-top breccia matrix (Δ), and an altered white massive

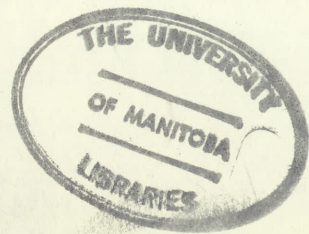


Thesis
H 226

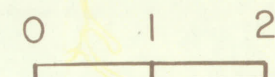
Plate 4. Outcrop diagram showing pillowed flow 10 underlain and overlain by complex massive flows. S flow 10 vary in shape from apparently discrete to interconnected. An exceptionally large pillow advancing flow. Its thickness exceeds that of some massive flows. Note the alteration within and at

Legend

- === Flow contact; approximate
- Sub-facies contact; approximate
-  Basal chill zone
-  Flow-top breccia
-  'Incomplete' pillow selvage
- Interpillow void
-  Light green weathering alteration
- ⊙ Limit of Outcrop
- ⊥ Overburden



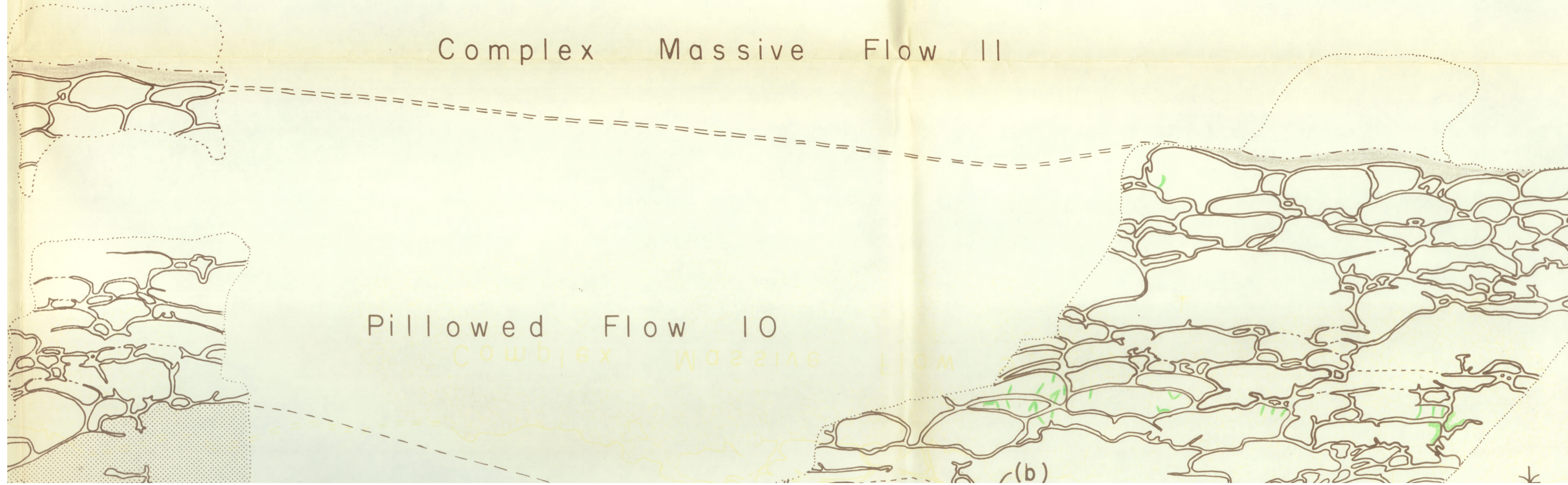
Geology by R. Hargreaves, 1975.



9 and 11 respectively. Only the flow-top breccia (patterned) of flow 9 is shown and has a relatively flat top. The pillows in flow-like body (a) at the base of the flow may represent part of the feeder system that supplied lava to the front of the flow. At the base of the pillowed flow and the incomplete selvages (b) between adjacent pillows.

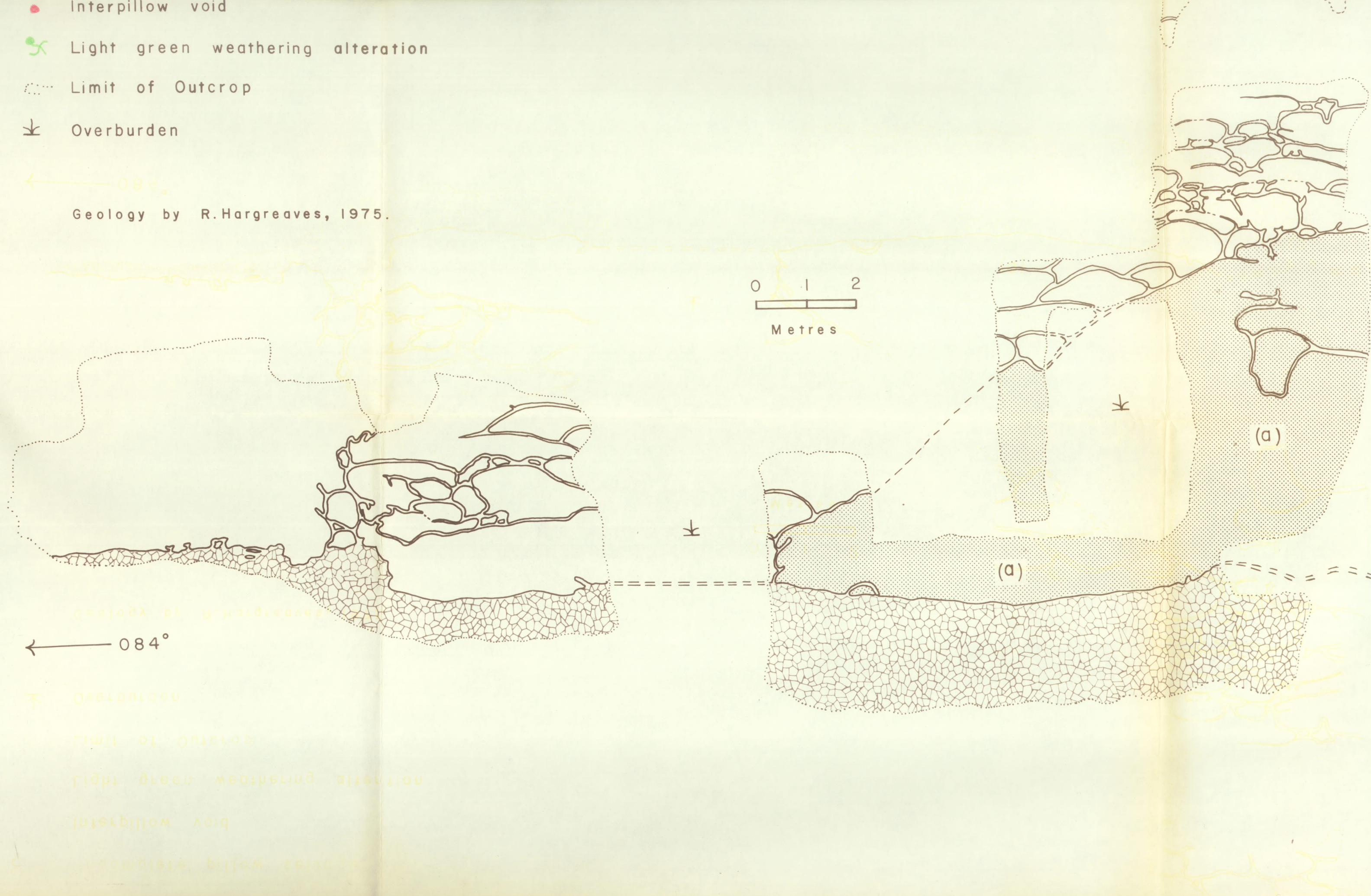
Complex Massive Flow 11

Pillowed Flow 10



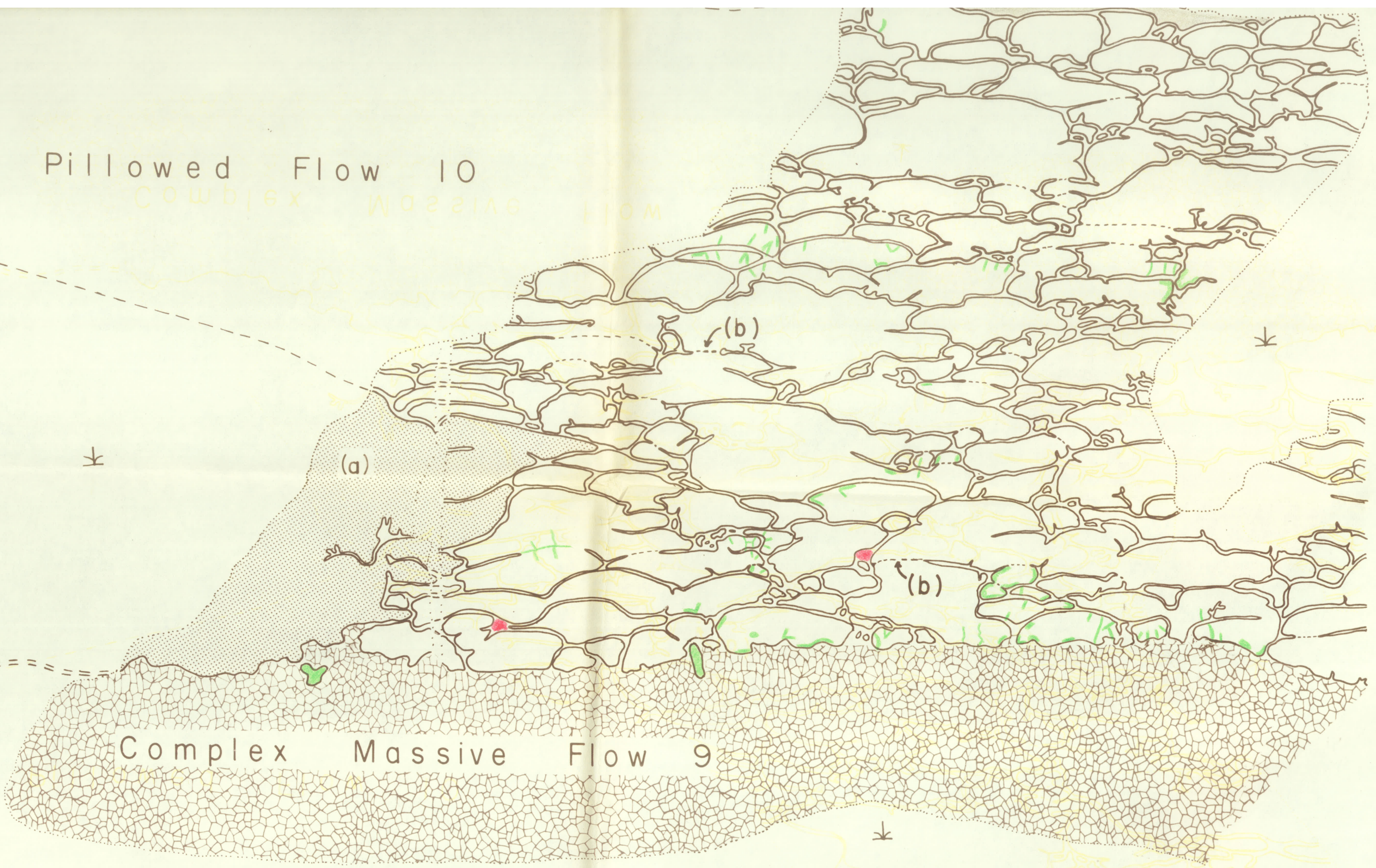
- Interpillow void
- ✕ Light green weathering alteration
- ⋯ Limit of Outcrop
- ⌞ Overburden

Geology by R.Hargreaves, 1975.



Pillowed Flow 10

Complex Massive Flow



Complex Massive Flow 9

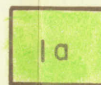
Legend



Metagabbro

————— Intrusive contact —————

Metabasalt flows; non-foliated, light to dark green in colour



Pillowed flow



Simple massive flow



Complex massive flow



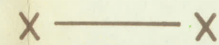
Symbols



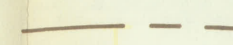
Pl. 2 Location of detailed outcrop maps



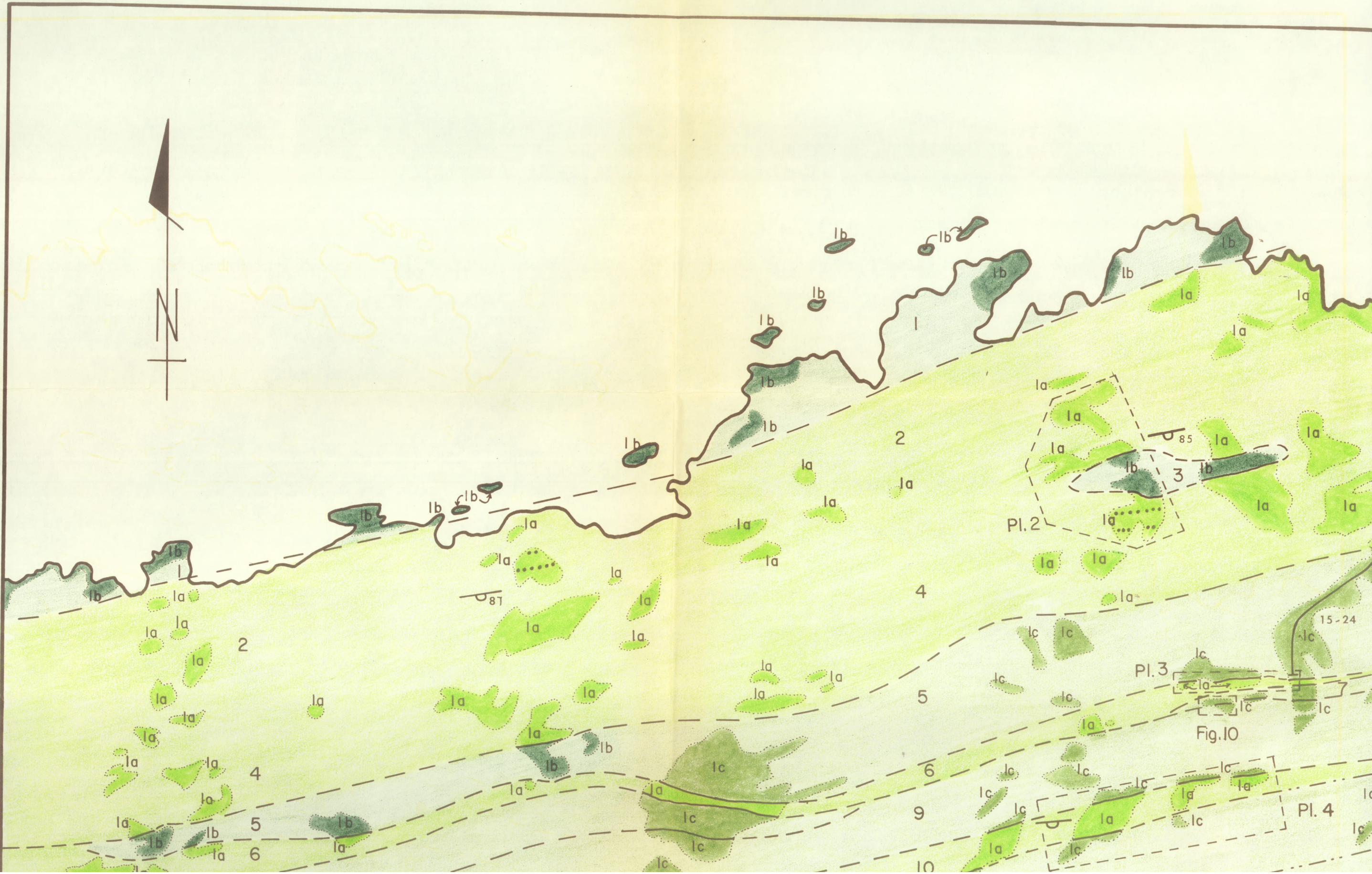
Lateral alteration zones; within pillowed flow units



Intrusive contact; approximate



Flow contact; defined, approximate, assumed

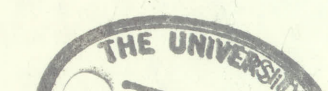


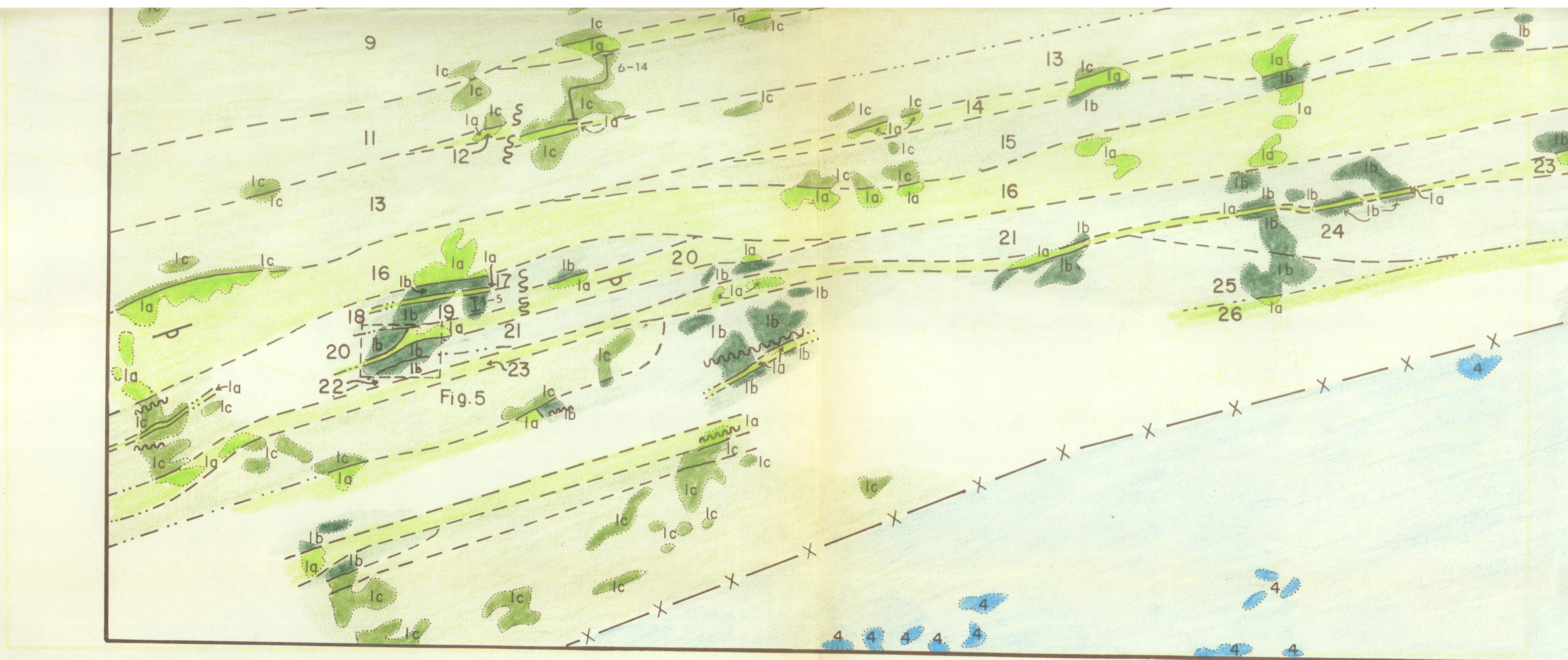


- dip unknown
- Fault; defined, assumed
- Location of chemical samples
- Outcrop
- Chronological order of flows
- Base map constructed from specially flown 1:4000 air photographs

Geology by R. Hargreaves, 1974, 1975 and 1976

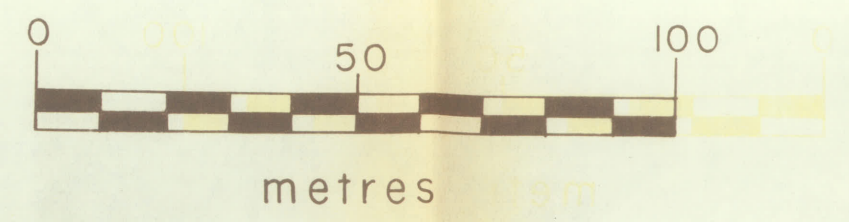
Utik Lake, Manitoba

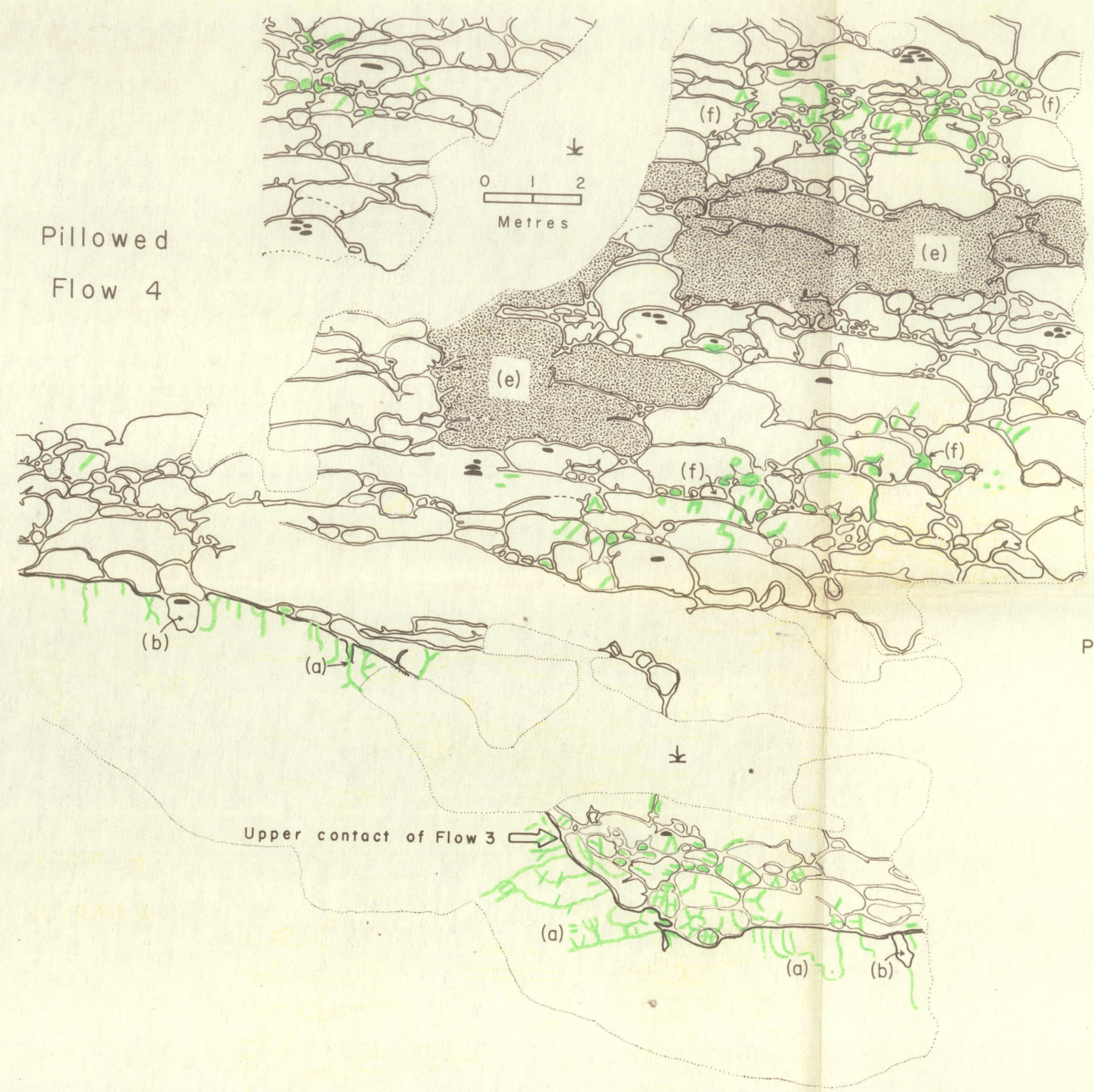




The Stratigraphy Of North-Central Mistuhe Island, Utik Lake, Manitoba

Horizontal Scale





Pillowed
Flow 4

Upper contact of Flow 3

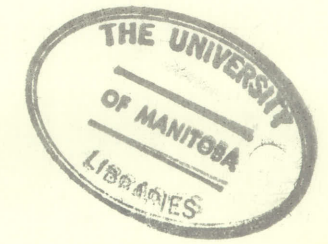
← 084°






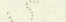
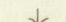
- Legend
- 'Incomplete' pillow selvage
 - Quartz-filled intrapillow cavity
 - Interpillow void
 - Calcite-filled interpillow void
 - Light green weathering alteration
 - Limit of outcrop

Simple Massive Flow 3

Plate 2. Outcrop diagram of simple massive flow 3 which is underlain and overlain by pillowed flows 2 and 4 respectively. Flow 3 has an undulating base. The flow surface is smooth and inclined, containing altered subvertical cooling cracks (a) and local pillows within larger cracks (b). Most pillows in flow 2 appear as discrete individuals, and may contain one or more intrapillow cavities. Such cavities occur in the more rounded pillows and are generally confined to distinct lateral zones within (c) and on top of (d) the flow. Pillows in flow 4 are more irregular in shape than in flow 2. Note the large, irregular, interconnected pillows (e) and the lateral zones of probable ocean-water alteration (f) within flows 2 and 4.

Dep Col
Thesis
H 226

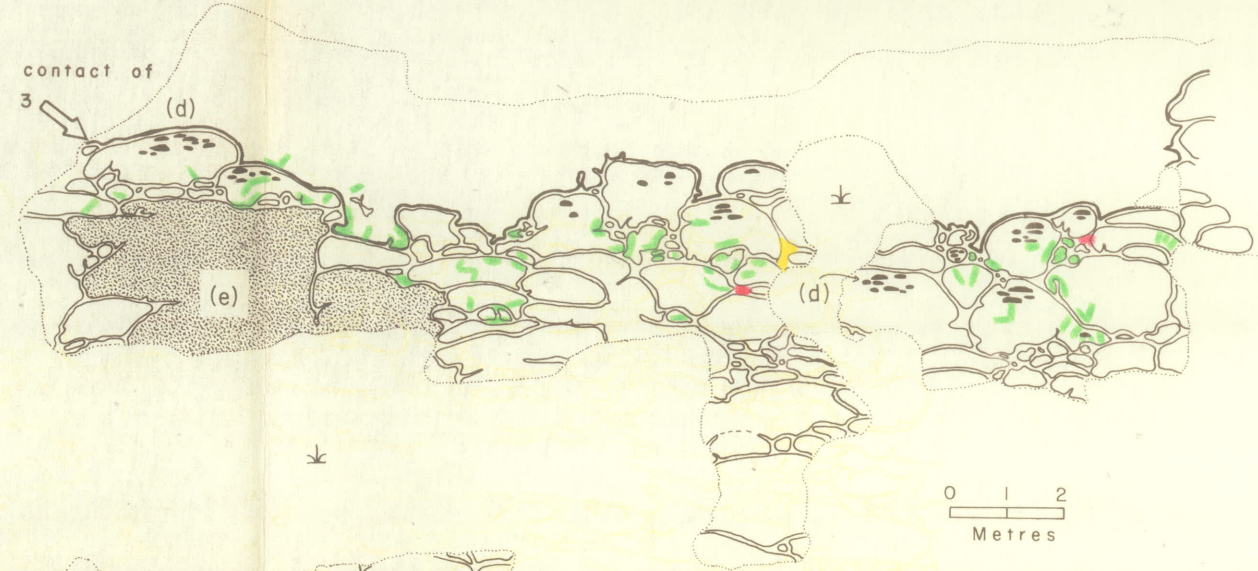


-  'Incomplete' pillow selvage
-  Quartz-filled intrapillow cavity
-  Interpillow void
-  Calcite-filled interpillow void
-  Light green weathering alteration
-  Limit of outcrop
-  Overburden

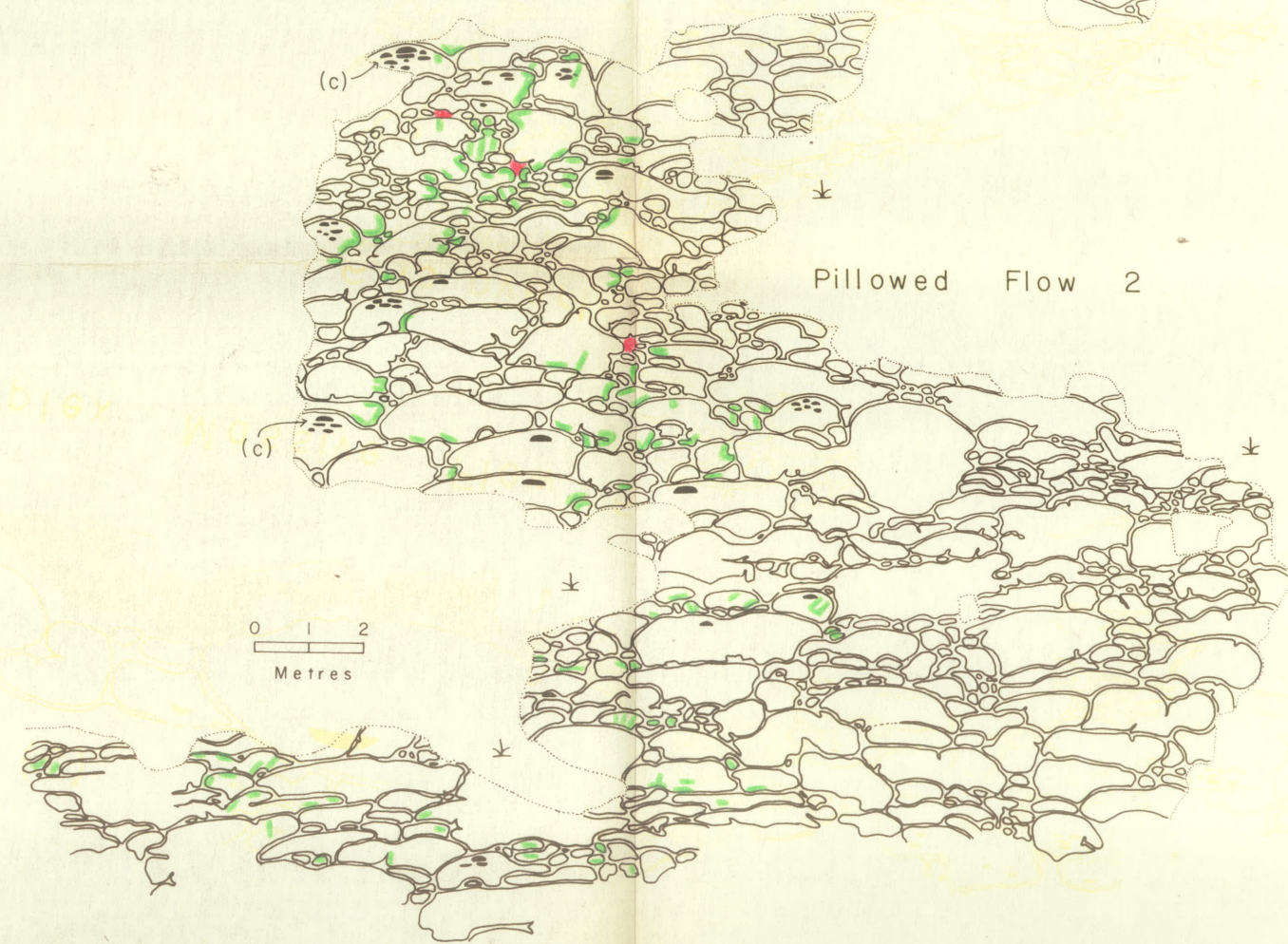
Geology by R. Hargreaves, 1975.

Simple Massive Flow 3

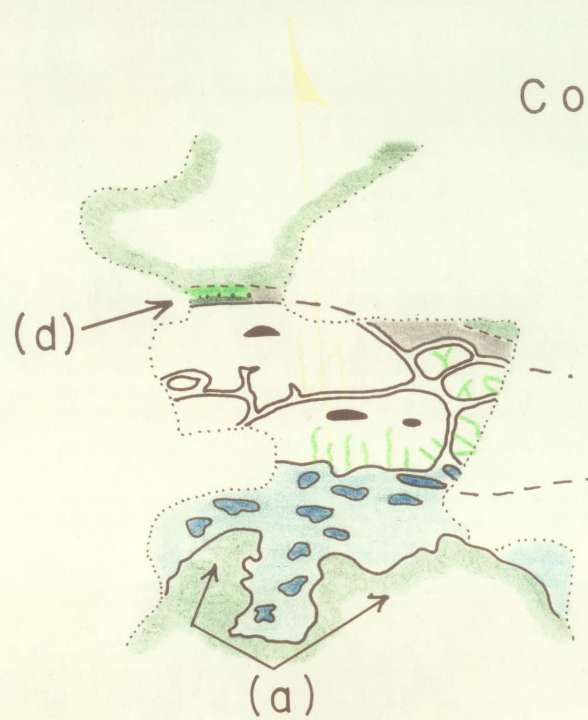
Basal contact of Flow 3



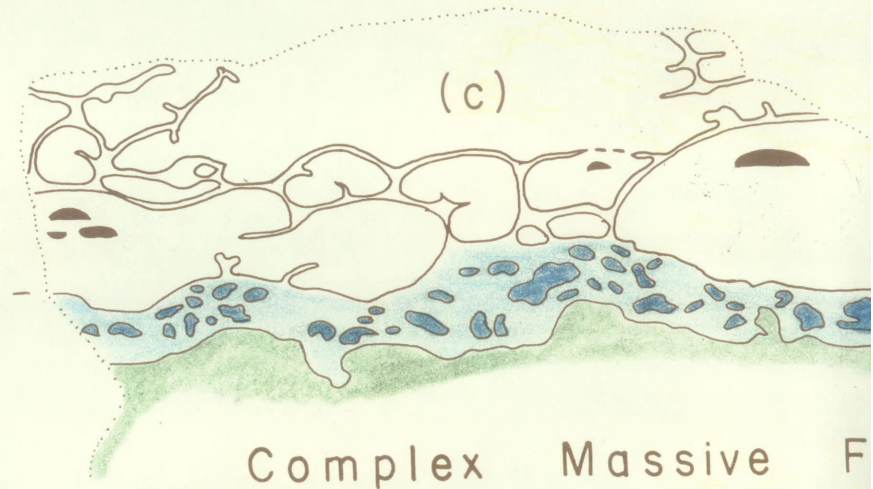
Pillowed Flow 2



Complex Massive Flow 7



Pillowed Flow 6



Legend

- Flow contact; approximate, assumed
- ▬ Basal chill zone
- ⌒ 'Incomplete' pillow selvage
- ◐ Intrapillow cavity
- ✕ Light green weathering alteration
- ⋈ Limit of outcrop
- ⌞ Overburden

0 1 2
Metres



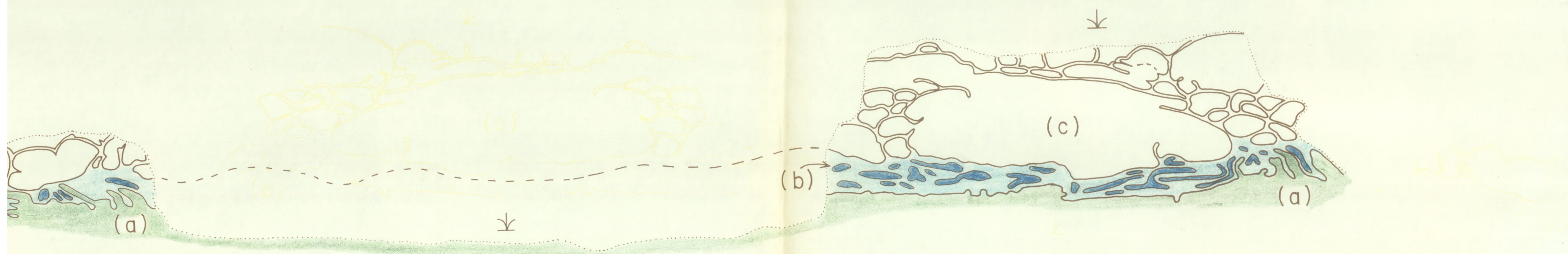
Geology by R. Hargreaves, 1975, 1976.

Plate 3. Pillowed flow 6 is overlain by Complex Massive Flow 7 (dark blue) at its surface. No pillows are interconnected by dark green laminae (d). Pillows have intrapillow cavities.



Massive Flow 5

Flow 6 is overlain and underlain by complex massive flows. Flow 5 has a slightly undulating flow-top breccia (light blue) on its surface. Note the massive protrusions (a) and altered white massive basalt blocks (b) within the breccia. Some of these blocks are interconnected (c) and contain intrapillow cavities. Flow 7 has a basal chilled zone that locally contains alternating light and dark laminae (d). Pillowed flow 6 gradually thins eastward, and eventually terminates east of the area shown here.



underlain by complex massive flows. Flow 5 has a slightly undulating flow-top breccia (light and
 protrusions (a) and altered white massive basalt blocks (b) within the breccia. Some of the
 intrapillow cavities. Flow 7 has a basal chilled zone that locally contains alternating light and
 gradually thins eastward, and eventually terminates east of the area shown here.